J|A|C|S
ARTICLES
Published on Web 03/18/2004

The α-Helical Peptide Nucleic Acid Concept: Merger of Peptide Secondary Structure and Codified Nucleic Acid Recognition

Yumei Huang,[†] Subhakar Dey,[†] Xiao Zhang,[†] Frank Sönnichsen,[‡] and Philip Garner*,[†]

Contribution from the Department of Chemistry and Department of Physiology and Biophysics, Case Western Reserve University, Cleveland, Ohio 44106-7078

Received September 10, 2003; E-mail: ppg@case.edu

Abstract: A novel platform for nucleic acid recognition that integrates the α-helix secondary structure of peptides with the codified base-pairing capability of nucleic acids is reported. The resulting α-helical peptide nucleic acids (αPNAs) are composed of a repeating tetrapeptidyl unit, aa_1-aa_2-aa_3-Ser^B, where aa_1 through aa_3 represent generic ancillary amino acids and B = nucleobases linked to Ser via a methylene bridge. Effective syntheses of constituent Fmoc-protected nucleoamino acids (Fmoc-Ser^B-OH, where B = thymine, cytosine, and uracil) are described along with a protocol for the solid-phase synthesis of 21mer αPNAs containing five such nucleobases. By varying the ancillary amino acids, two distinct classes of αPNAs were constructed, having a net charge of −1 or +6, respectively, at physiological pH. The modular nature of the αPNA platform was illustrated by the synthesis of symmetrical disulfide-bridged αPNA dimers containing 10 nucleobases. Hybridization of these αPNAs with ssDNA has been examined by thermal denaturation, gel electrophoresis, and circular dichroism (CD) and the data indicated that αPNA binds to ssDNA in a cooperative manner with high affinity and sequence specificity. In general, b2 αPNAs bind faster and more strongly with ssDNA than do the corresponding b1 αPNAs. Parallel αPNA−DNA complexes are more stable than their antiparallel counterparts. CD studies also revealed that the hybridization event involves the folding of both species into their helical conformations. Finally, NMR experiments provided conclusive evidence of Watson−Crick base pairing in αPNA−ssDNA hybrids.

Introduction

The seminal discovery[1] that translation can be inhibited by an antisense oligonucleotide (oligo) suggested a general approach to therapeutic intervention.[2] The related phenomenon of RNA interference (RNAi)[3] involves the generation of an antisense RNA complexed to a protein with RNase activity.[4] Currently, phosphorothioate oligodeoxynucleotides (PS ODNs) and 2′-*O*-(2-methoxyethyl)-modified PS ODNs represent the state-of-the-art in antisense technology.[5] Although drugs based on PS ODNs have reached the marketplace, there are drawbacks associated with the current technology. For one thing, PS oligos are not trivial to prepare in stereochemically homogeneous form and are, therefore, formulated as mixtures of diastereomers. The specificity of PS oligos may be compromised by their RNase-based mechanism of action if degradation of partially complementary nontarget mRNA sequences occurs. Furthermore, PS oligos are known to interact with proteins,[6] and this may lead to unintended side effects. One solution to this collection of problems involves replacing the repeating ribose phosphate with a simpler and more versatile backbone. Morpholino oligos (which are, in fact, derived from ribonucleotides) represent one such backbone replacement.[7] Despite their ability to inhibit translation in cell-free experiments, morpholino oligos are not taken up into cells efficiently.[8]

Yet another approach involves the use of a peptide or peptide-like backbone. Even though peptide and peptide-like nucleic acid surrogates were first proposed some 30 years ago,[9,10] a successful antisense drug based on this class of hybrid molecules has yet to emerge. Of the many structural motifs examined, Nielsen's peptide nucleic acid (PNA) has come the closest to

[†] Department of Chemistry.
[‡] Department of Physiology and Biophysics.

(1) Zamecnik, P. C.; Stephensen, M. L. *Proc. Natl. Acad. Sci. U. S A.* **1978**, *75*, 280.
(2) (a) *Antisense Technology Part A: General Methods, Methods of Delivery and RNA Studies*; Phillips, M. I., Ed.; Academic Press: San Diego, CA, 2000; Methods in Enzymology, Vol. 313. (b) *Antisense Technology Part B: Applications*; Phillips, M. I., Ed.; Academic Press: San Diego, CA, 1999; Methods in Enzymology, Vol. 314;
(3) Fire, A.; Xu, S.; Montgomery, M. K.; Kostas, S. A.; Driver, S. E.; Mello, C. C. *Nature* **1998**, *391*, 806.
(4) Hutvágner, G.; Zamore, P. D. *Science* **2002**, *297*, 2056.
(5) Crooke, S. T., Ed. Antisense Drug Technology − Principles, Strategies and Applications; M. Decker: New York, 2001.
(6) King, D. J.; Ventura, D. A.; Brasier, A. R.; Gorenstein, D. G. *Biochemistry* **1998**, *37*, 16489.
(7) Summerton, J.; Weller, D. *Antisense Nucleic Acid Drug Dev.* **1997**, 2375, 187.
(8) Summerton, J.; Stein, D.; Huang, S.; Matthews, P.; Weller, D.; Partridge, M. *Antisense Nucleic Acid Drug Dev.* **1997**, *7*, 63.
(9) (a) de Koning, H.; Pandit, U. K. *Rec. Trav. Chim.* **1971**, *91*, 1069. (b) Buttrey, J. D.; Jones, A. S.; Walker, R. T. *Tetrahedron* **1975**, *31*, 73. (c) Shvachkin, Yu. P. *Zh. Obshch. Khim.* **1979**, *49*, 1157.
(10) For a comprehensive compilation of peptide-based nucleic acid surrogates up to 1999, see: Falkiewicz, B. *Acta Biochim. Pol.* **1999**, *43*, 509. (See also ref 15).

10.1021/ja038434s CCC: $27.50

reaching this goal. This oligonucleotide surrogate stands out in terms of its structural simplicity and ability to bind sequence specifically to ssRNA and DNA.[11] In these systems, the ribose phosphate backbone is replaced by a repeating *N*-(2-aminoethyl)glycine unit,[12] which simplifies their synthesis and imparts biostability to the resulting oligomers. However, the first generation Nielsen PNAs have drawbacks associated with them (low solubility, insufficient orientation discrimination, poor cellular uptake) that have hindered their therapeutic application. The incorporation of chiral amino acids (D-Lys for example)[13] in place of glycine represents a possible solution to such problems, but the extent that one can actually functionalize the PNA backbone appears to be limited. One can add property-modifying functionality via conjugation (PNA−peptide or PNA−DNA chimerae);[14] however, this is done at the expense of increasing molecular complexity.

The ability to alter a molecule's chemical, biochemical, and/or pharmacological properties while maintaining its receptor binding affinity and specificity lies at the heart of successful drug development. Thus, it can be argued that the ideal antisense drug platform would consist of the simplest possible molecular framework that allows one to introduce functionality independent of the primary mRNA binding "domain". This line of reasoning led us to revisit the idea of replacing the ribose phosphate backbone with a peptide that has nucleobases attached to specific amino acid residues. It was surmised that the problem with earlier peptide-based nucleic acid surrogates (including one of our own design)[15] was due to improper spacing of the nucleobases. The peptide backbone in these systems would have to adopt an energetically unfavorable conformation to form Watson−Crick base-pairs with the target nucleic acid. We now present a full account of our successful development of a new synthetic construct that merges the α-helix secondary structure of peptides with the codified base-pairing capability of nucleic acids.[16,17]

Results and Discussion

1. Design Concept. The basic α-helical peptide nucleic acid concept is illustrated in Figure 1.[18] Our prototype αPNA module incorporated five nucleobases for Watson−Crick (W•C) base pairing with a single-stranded nucleic acid target. These nucleobases are attached to the peptide backbone via a flexible methylene linker to serine in order to preserve the *N*-glycoside (O−C−N) substructure found in nucleic acids.[19] We initially considered the tetrad or (i, $i + 4$) peptide spacing motif. In tetrad αPNAs made up of L-amino acids, the nucleobase-containing residues which are three amino acids apart trace a right-handed superhelix that can become aligned by tightening the α-helix to a 3_{10} helix. Assuming that the αPNA has a helical pitch of 5−6 Å, synchronized tilting of the nucleobases relative to the α-helix axis would be necessary to approximate the nucleobase spacing of a single-stranded nucleic acid in a standard B-helical geometry. In our αPNA, the flexible $-CH_2-O-CH_2-$ linker acts as a hinge for this purpose. This, along with the known deformability of both DNA and peptide α-helices,[20] was expected to lead to an induced fit driven by Watson−Crick base-pairing.

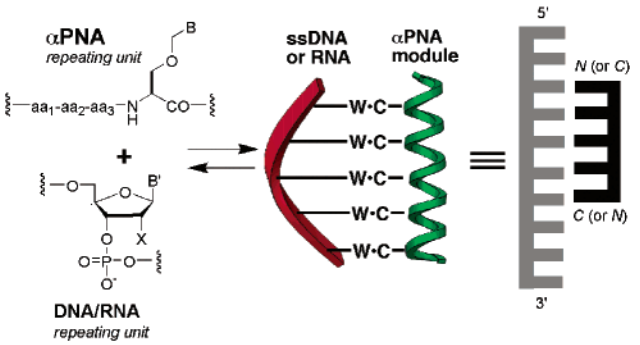

Figure 1. The αPNA design concept.

With the general αPNA design concept formulated, we next turned to the question of what ancillary amino acids should be incorporated into the peptide backbone. The goal was to minimally edit a known peptide sequence that favors α-helix formation. Our first αPNA (which we term backbone 1 or b1) was based on an amphipathic helix sequence emanating from Baltzer's group.[21] Specifically, this αPNA backbone included hydrophobic amino acids (Ala and Aib), internal salt bridges (Glu-$(aa)_3$-Lys-$(aa)_3$-Glu), a macrodipole (Asp-$(aa)_{15}$-Lys), and an *N*-acetyl cap to favor α-helix formation.[22] The C-termini of these αPNA modules end in a carboxamide function to preclude any potential intramolecular end effects (Figure 2). The incorporation of a Cys residue at position 21 allowed for implementation of Goddard's "disulfide stitchery" strategy[23] to connect two b1 αPNA modules at the N-terminus. Replacement of Gly1 with Cys and Cys21 with Aib provided b1′ αPNAs for connection at the C-terminus. We decided on a disulfide linkage first to demonstrate the modular nature of our platform, even though the resulting αPNA-dimers would probably not be suitable drug candidates due to the ease of reductive disulfide cleavage in the cytoplasm.

While the binding properties of backbone 1 αPNAs with complementary ssDNAs were being studied, it was discovered

(11) (a) Nielsen, P. E.; Egholm, M.; Berg, R. H.; Buchhardt, O. *Science* **1991**, *254*, 1497. (b) Egholm, M.; Buchhardt, O.; Nielsen, P. E.; Berg, R. H. *J. Am. Chem. Soc.* **1992**, *114*, 1895. (c) For a comprehensive review, see: Uhlmann, E.; Peyman, A.; Breipohl, G.; Will, D. W. *Angew. Chem., Int Ed.* **1998**, *37*, 2796n.

(12) The idea of using *N*-(2-aminoethyl)glycine as a ribose phosphate replacement may actually be traced back to an article by Westheimer. See: Westheimer, F. H. *Science* **1987**, *235*, 1173.

(13) (a) Sforza, S.; Haaima, G.; Marchelli, R.; Nielsen, P. E. *Eur. J. Org. Chem.* **1999**, 197. (b) Sforza, S.; Corradini, R.; Ghirardi, S.; Dossena, A.; Marchelli, R. *Ibid*. **2000**, 2905.

(14) Uhlmann, E.; Peyman, A.; Breipohl, G.; Will, D. W. *Angew. Chem., Int. Ed.* **1998**, *37*, 2796.

(15) Garner. P.; Yoo, J. U. *Tetrahedron Lett.* **1993**, *34*, 1275.

(16) Preliminary accounts of this work: (a) Garner, P.; Dey, S.; Huang, Y.; Zhang, X. *Org. Lett.* **1999**, *1*, 403. (b) Garner, P.; Dey, S.; Huang, Y. *J. Am. Chem. Soc.* **2000**, *122*, 2405.

(17) After our original αPNA communication appeared (ref 16a), Mihara and co-workers reported the incorporation of nucleobase-containing amino acids into both coiled-coils and α-helical peptides designed to recognize HIV-1 RRE RNA: (a) Matsumura, S.; Ueno, A.; Mihara, H. *Chem. Commun.* **2000**, 1615. (b) Takahashi, T.; Hamasaki, K.; Ueno, A.; Mihara, H. *Bioorg. Med. Chem.* **2001**, *9*, 991.

(18) Amino acid abbreviations: aa = generic amino acid, Ala = L-alanine, Aib = 2-aminoisobutyric acid, Cys = L-cysteine, Asp = L-aspartic acid, Glu = L-glutamic acid, Gly = glycine, Lys = L-lysine, Ser = L-serine, Ser^T = (*S*)-2-amino-3-(5-methyl-2,4-dioxo-3,4-dihydro-2*H*-pyrimidin-1-ylmethoxy)propionic acid, Ser^C = (*S*)-2-amino-3-(4-amino-2-oxo-2*H*-pyrimidin-1-ylmethoxy)propionic acid, Ser^U = (*S*)-2-amino-3-(2,4-dioxo-3,4-dihydro-2*H*-pyrimidin-1-ylmethoxy)propionic acid.

(19) The synthesis of racemic Bz-Ser^U-OMe was reported in the Russian chemical literature in another context: Timoshchuk, V. A.; Olimpieva, T. I. *Zhurnal Obshei Khimii* **1988**, *58*, 2404.

(20) Curran, T.; Kerppola, T. K. *Science* **1991**, *254*, 1210.

(21) (a) Olofsson, S.; Johansson, G.; Baltzer, L. *J. Chem. Soc., Perkin Trans. 2*. **1995**, 2047. (b) Broo, K. S.; Brive, L.; Ahlberg, P.; Baltzer, L. *J. Am. Chem. Soc.* **1997**, *119*, 11362.

(22) Regan, L.; Degrado, W. F. *Science* **1988**, *241*, 976.

(23) Park, C., Campbell, J. L.; Goddard, W. A., III. *J. Am. Chem. Soc.* **1995**, *117*, 6287.

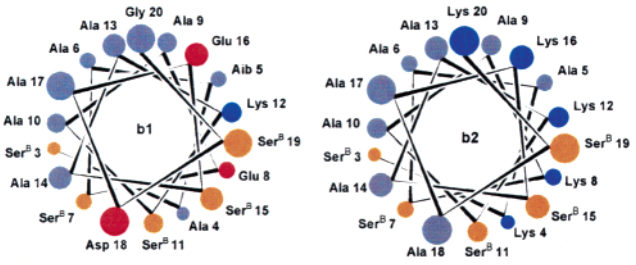

Figure 2. Helical-wheel representations of backbone 1 and 2 αPNAs. b1 sequence: Ac-Cys^{Acm}-Gly-Ser^B-Asp-Ala-Glu-Ser^B-Ala-Ala-Lys-Ser^B-Ala-Ala-Glu-Ser^B-Ala-Aib-Ala-Ser^B-Lys-Gly-NH$_2$. b2 sequence: Ac-Cys^{Acm}-Lys-Ser^B-(Ala-Ala-Lys-Ser^B)$_4$-Gly-Lys-NH$_2$.

that the rate of association was extremely slow even though the resulting αPNA−ssDNA complexes were relatively stable. We hypothesized that at neutral pH, b1 αPNAs were negatively charged, thereby introducing a kinetic barrier to the process of association with negatively charged ssDNA. It was surmised that if one could make αPNAs that were positively charged at neutral pH, this kinetic barrier could be reduced by virtue of attractive Coulombic forces. In this context, it had been reported that the attachment of a positively charged Lys-rich peptide to DNA enhanced the rate of duplex formation 48 000-fold.[24] A new backbone was designed based on the simple logic of replacing the negatively charged Asp and Glu residues in b1 with Ala and positively charged Lys residues, respectively. Additional Lys residues were incorporated at Ala4 and Gly20, and the Aib residue was replaced by Ala. Finally, the Gly1 and Lys2 residues were interchanged in order to avoid proximal Lys residues. The resulting backbone 2 or b2 αPNAs (Figure 2) would now have a net charge of +6 at neutral pH. N-Terminal dimerization of b2 αPNAs was possible via the Cys21 residue. For dimerization at the C-terminus, the Lys1 and Cys21 residues were interchanged to give the b2′ αPNA backbone motif.

2. αPNA Synthesis. 2a. Nucleoamino Acid Synthesis. Thymine, cytosine, and uracil containing N^{α}-9-fluorenylmethoxycarbonyl (Fmoc)-protected nucleoamino acids **6**, **10**, and **13** were synthesized (Scheme 1) by a modification of the route we used to prepare the analogous *tert*-butoxycarbonyl (Boc)-protected species (see ref 15). The Fmoc group was to be incorporated at the very beginning of the synthesis. The exocyclic amine group of the cytosine was to be protected with the acid-labile Boc group, which can be cleaved at the end of the αPNA synthesis under mildly acidic (or even neutral)[25] conditions, thus minimizing the exposure of the αPNAs to acid. The carboxylic acid moiety was to be masked as its benzyl ester, which can be cleaved under neutral hydrogenolysis conditions at the end of the nucleoamino acid synthesis. Both the acid (Boc)- and base (Fmoc)-sensitive functionality were to be retained in a way that would not jeopardize the configurational stability of the nucleoamino acid building blocks.

The first task was to synthesize the methylthiomethyl (MTM) ether **3** on a large scale, using the minimum number of steps from a commercially available starting material. Fmoc-Ser-OH **1** was chosen as the starting material and is a relatively inexpensive commercially available chemical. The carboxylic acid group of **1** was protected as a benzyl ester using benzyl bromide in the presence of tetrabutylammonium iodide and $KHCO_3$ in DMSO. Alcohol **2** was smoothly converted to the MTM ether **3** in high yield via a Pummerer-like reaction using benzoyl peroxide and dimethyl sulfide in acetonitrile.[26] It is worth mentioning here that the analogous MTM ether in the Boc series was obtained as an oil and was difficult to purify by flash chromatography. On the other hand, the Fmoc derivative **3** is a crystalline solid and is easy to purify using flash column chromatography. This common intermediate **3**, available in one step from commercially available **2**, was used to synthesize all of the nucleoamino acids.

Following Sugimura's lead,[27] *N*-bromosuccinimide (NBS) was initially chosen as the promoter for the nucleosidation reaction between bis-silylated thymine **4**[28] and MTM ether **3**. A mixture of the desired product **5** along with its N^3 regioisomer (not shown) was obtained in about a 1.2:1 ratio. Both Ogilvie[29] and Tsantrizos[30] reported that only one regioisomer (N^1) formed when I_2 was used as an activator with similar MTM ether substrates. Using this activator, a single product was obtained in 60% yield (95% based on recovered **3**). The reaction profile depends on various factors. One of them is the relative concentration of I_2 over **3**, the optimal I_2/**3** ratio being 1.5. A mixture of N^1 and N^3 regioisomers formed if over 2.0 equiv of I_2 was used or if the reaction time was extended beyond 48 h. Also, when I_2 was added to the reaction mixture before bis-silylated thymine, **3** is converted to two (unidentified) side products and **5** is not formed. Hydrogenolytic deprotection of the benzyl ester using H_2 and Pd−C (10%) in THF−MeOH was clean, providing the thymine-containing nucleoamino acid **6** in quantitative yield.

For the incorporation of cytosine into our αPNA, it was decided to protect the N^4-amino group. The Boc group was chosen for this purpose because it's reactivity is orthogonal to the Fmoc protecting group. Cytosine was treated with Boc_2O and a catalytic amount of DMAP, to give pure N^4-Boc cytosine **7** in 54% yield after a simple workup. The mono-silylated 2-trimethylsilyl-N^4-Boc-cytosine **8** undergoes reaction with **3** in the presence of I_2 to produce the desired compound **9** as single isomer in 46% isolated yield (96% based on recovered 3).[31] Clean removal of the benzyl group was observed when 10 equiv of 1,4-cyclohexadiene was used along with 10% Pd−C in THF−MeOH (1:1) as solvent.[32] The cytosine-containing nucleoamino acid **10** was thus obtained as a pure solid in quantitative yield.

Following a similar procedure, the uracil nucleoamino acid was synthesized. Only one major compound **12** was obtained in 24% isolated yield (74% based on recovered **3**) from the iodine-mediated reaction of **3** and U·2TMS[33] **11**. 1,4-Cyclohexadiene-mediated benzyl group cleavage gave **13** in quantitative yield.

(24) Corey, D. R. *J. Am. Chem. Soc.* **1995**, *117*, 9373.
(25) (a) Hwu, J. R.; Jain, M. L.; Tsay, S.-C.; Hakimelahi, H. *Tetrahedron Lett.* **1996**, *37*, 2035. (b) Siro, J. G.; Martín, J.; García, J. L.; Remuiñan, M. J.; Vaquero, J. J. *Synlett* **1998,** 147. (c) Ham, J.; Choi, K.; Ko, J.; Lee, H.; Jung, M. *Protein Pept. Lett.* **1998**, *5*, 257.
(26) Median, J. C.; Salomon, M.; Kyler, K. S *Tetrahedron Lett.* **1988**, *29*, 3773.
(27) Sugimura, H.; Osumi, K.; Kodaka, Y.; Sujino, K. *J. Org. Chem.* **1994**, *59*, 7653.
(28) Garner, P.; Park, J. M. *J. Org. Chem.* **1990**, *55*, 3772.
(29) Ogilvie, K. K.; Nguyen-Ba, N.; Hamilton, R. G. *Can. J. Chem.* **1984**, *62*, 1622.
(30) Tsantrizos, Y. S.; Lunetta, J. F.; Boyd, M.; Fader, L. D.; Wilson, M. C. *J. Org. Chem.* **1997**, *62*, 5451.
(31) Huang, Y.; Dey, S.; Garner, P. *Tetrahedron Lett.* **2003**, *44*, 1441.
(32) Bajwa, J. S. *Tetrahedron Lett.* **1992**, *33*, 2299.
(33) Cheng, V.; Hughes, L.; Griffin, V. B.; Montserret, R.; Ollapally, A. P. *Nucleosides Nucleotides* **1986**, *5*, 223.

Scheme 1. Synthesis of Nucleoamino Acids. The Atom Designation Scheme Shown for Compound **5** Is General for All Nucleoamino Acids

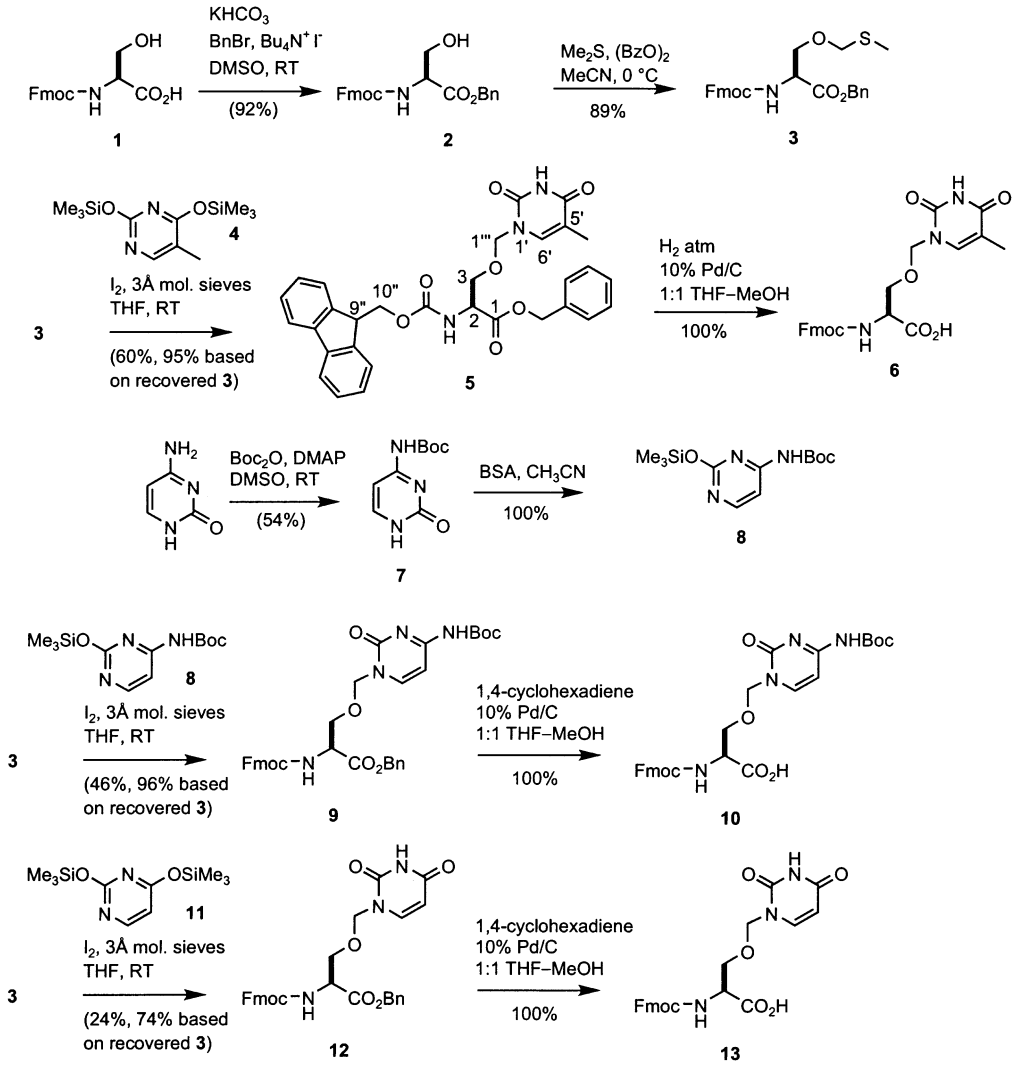

The N^1 and N^3 isomers of the thymine derivatives can often be distinguished by analyzing the peak-shape of the H-6′ signal in ^{1}H NMR spectrum. The N^1 isomer is expected to give a singlet while a doublet or broad singlet is expected for the N^3 isomer due to adjacent NH proton coupling. However, this simple analysis was not possible with the Fmoc-thymine nucleoamino acid **6**. Correlation of ^{13}C NMR data (C-5′ and C-6′) with that of similar pyrimidine derivatives can be used to assign regiochemistry.[34] However, such assignments are not unambiguous—especially when only one regioisomer is available. Since there was precedent for determining nucleobase regiochemistry using two-dimensional long-range heteronuclear multiple bond shift correlation (HMBC) NMR experiments, we decided to apply this method to our system.[35] The protecting groups of the pyrimidine nucleoamino acids were removed by treatment with 2% DBU in DCM followed by 95% TFA in water. Assignments of the proton-attached carbons were made via the heteronuclear multiple-quantum coherence (HMQC) experiments of these compounds. Subsequent HMBC experiments showed that the thymine-, cytosine-, and uracil-containing nucleoamino acids possess the HMBC patterns expected of the N^1 regioisomer (Figure 3).

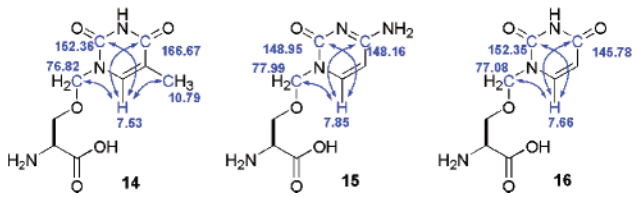

Figure 3. HMBC correlation of H-Ser^T-OH **14**, H-Ser^C-OH **15**, and H-Ser^U-OH **16** regiochemistry.

2b. **Solid-Phase αPNA Synthesis.** Our general synthetic route to αPNAs and their symmetrical disulfide dimers is depicted in Scheme 2. The synthesis consisted of three distinct stages: (1) solid-phase αPNA synthesis of the resin-bound module **18**, (2) cleavage of the peptides from the resin with concomitant global deprotection of all amino acid residues except Cys to give αPNA module **19**, and (3) thiol deprotection and disulfide bond formation to produce the symmetrical dimer **20**. Because the nucleobase-containing serine residue is potentially both acid- and base-labile, the strategic and tactical issues associated with the solid-phase synthesis of these αPNAs

(34) Kalinowski, H. O.; Berger, S.; Braun, S. *Carbon-13 NMR Spectroscopy*; Translated by Becconsall, J. K. Imprint Chichester; Wiley: New York, 1988; pp 441.

(35) (a) Bax, A.; Summers, M. F. *J. Am. Chem. Soc*. **1986**, *108*, 2093. (b) Huang, J. J.; Ragouzeos, A.; Rideout, J. L. *J. Heterocycl. Chem*. **1994**, *31*, 1685. (c) Timár, Z.; Kovács, L.; Kovács, G.; Schmél, Z *J. Chem. Soc., Perkin Trans*. **2000**, *1*, 19.

Scheme 2. Solid-Phase Synthesis of αPNA.

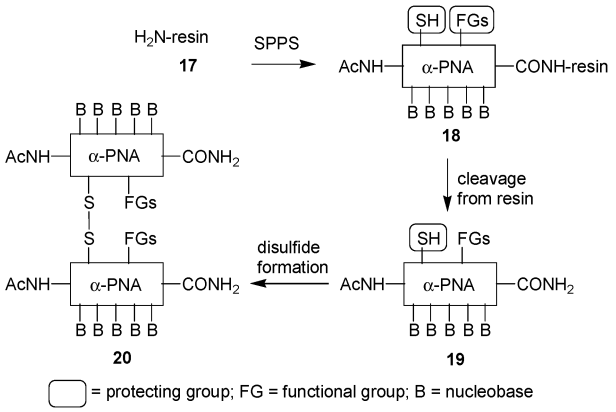

resemble those associated with glycopeptides.[36] Accordingly, we chose the commercially available Fmoc-Rink amide MBHA resin as the solid support. The base-labile Fmoc protecting group (PG) for the N-terminal amines and acid-labile PGs (Boc and *tert*-butyl ester) for all side chain functionality excepting Cys. The I_2-labile acetamidomethyl (Acm) PG was chosen for the Cys residue to facilitate a separate disulfide bond formation step.[37] DBU[38] was used for Fmoc deprotection, and Carpino's HATU[39] reagent was used for all peptide couplings (except that involving Fmoc-Cys^{Acm}-OH). Finally, the acid-labile Rink amide linker[40] permitted the release of a fully extended peptide amide from the resin and removal of the acid-labile PGs at the same time. Several homo and hetero pyrimidine base-containing αPNAs were synthesized using optimized protocol in about 20% overall average yield after preparative HPLC purification. An abasic peptide corresponding to b2 was also synthesized by replacing nucleoamino acids with Ser and was used as a control sequence for binding studies. αPNAs were characterized by either MALDI-TOF or ESI mass spectrometry (See Table S1 in Supporting Information).

2c. αPNA Dimer Formation. To assemble αPNA sequences containing more than five nucleobases, we joined two modules together using Goddard's "disulfide stitchery" strategy. Our b1 and b2 αPNAs incorporated a Cys residue at the N-terminus while the b1′ αPNA backbone had a Cys residue at the C-terminus. The plan was to use postpurification I_2-mediated dimerization of *S*-Acm protected αPNAs to obtain the αPNA dimers. In the event, exposure of the T_5(b1) monomer to a solution of I_2[41] in MeOH−H_2O provided the tail-to-tail T_5(b1)-dimer in 84% yield after HPLC purification. Similar treatment of T_5(b1) monomer resulted in a 49% purified yield of the head-to-head T_5(b1′)-dimer. However, when we applied these conditions to cytosine-containing backbone 2 αPNAs, the result was a complex reaction profile. It was hypothesized that the problem might be the oxidation of Lys side chains (or other amino groups) by I_2 during the dimerization reaction. This problem was circumvented by adjusting the pH so as to convert all of the free amines to their corresponding ammonium salts. Thus, when the reaction was performed in 0.5 M HCl, a clean conversion from monomer to dimer was observed. These symmetrical B10 αPNA dimers were characterized by MALDI-TOF or ESI mass spectrometry (See Table S2 in Supporting Information).

3. Binding Studies. Our αPNA−DNA binding studies addressed the following questions: (1) What is the stand alone conformation of αPNAs? (2) What is αPNA's capacity and propensity to hybridize with ssDNA? (3) Is there specific hydrogen bonding recognition between the nucleobases of DNA and αPNA? (4) What are the orientational specificity, stoichiometry, and conformation of such hybrids? Thermal denaturation, gel electrophoresis, circular dichroism, and NMR spectroscopy were used to study αPNA and DNA interactions. Two αPNA structural variants were studied, each differing in the overall charge of the peptide backbone. The αPNAs constitute both symmetrical (CCCCC, TTTTT, CCTCC) and asymmetric (CTCCT) nucleobase sequences.

3a. Thermal Denaturation Studies on αPNA−ssDNA Complexes. UV melting was used to evaluate the mutual affinity of αPNA and ssDNA. This method is based on the hyperchromic UV absorption shift of stacked versus unstacked base-pairs. Cooperative binding is generally indicated by a sigmoidal absorption versus temperature curve, with the transition midpoint being defined as the melting temperature (T_m). Comparison of the dissociation (heating) and association (cooling) curve can also provide a qualitative indication of the binding kinetics. T_m measurements on complexes with base-pair mismatches between αPNA and DNA provide information about the sequence specificity of binding.

DNA with dangling nucleobases (represented by italicized letters) on the 5′ and 3′ ends was initially used for the αPNA hybridization studies with $d(G)_5$ and $d(G)_{10}$ since DNAs made up of contiguous tracts of guanosine nucleotides tend to form aggregates in solution. The addition of the dangling bases at both ends of DNA was also reported to increase the T_m of the DNA duplex possibly through additional nonspecific interactions (hydrophobic packing, neighboring base stacking) or the exclusion of solvent intrusion into the terminal base-pairs.[42] Subsequently, we incorporated dangling bases into all of our ssDNA sequences.

The amino acid sequence of our first αPNA series (which we termed as backbone 1 or b1) was designed based on an amphipathic helix sequence (Ac-Cys^{Acm}-Gly-Ser^{B}-Asp-Ala-Glu-Ser^{B}-Ala-Ala-Lys-Ser^{B}-Ala-Ala-Glu-Ser^{B}-Ala-Aib-Ala-Ser^{B}-Lys-Gly-NH_2; represented as BBBBB(b1), where B is generic nucleobase). A characteristic sigmoidal curve was observed for a CCCCC(b1) + $d(TA_3G_5A_3T)$ (T_m = 34 °C) solution which was annealed in water for 4 days at 4 °C (Table 1, entry 3). This T_m value is indicative of the formation of a stable complex. However, no reassociation of the complex was observed during the cooling cycle. Both b1 (tail-to-tail T_m = 39 °C) and b1′ (head-to-head T_m = 51 °C) TTTTT dimers showed cooperative binding with $d(A_{10})$. Again no reassociation of the complex was observed during the cooling cycle. A T_m difference of approximately 12 °C was observed for b1 (tail-to-tail) and b1′

(36) Paulsen, H.; Schleyer, A.; Mathieux, N.; Meldal, M.; Bock, K. *J. Chem. Soc., Perkin Trans. 1* **1997**, 281.
(37) Veber, D. F.; Milkowski, J. D.; Varga, S. L.; Denkewalter, R. G.; Hirschmann, R. *J. Am. Chem. Soc.* **1972**, *94*, 5456.
(38) Wade, J. D.; Bedford, J.; Sheppard, R. C. Tregear, G. W. *Pept. Res.* **1991**, *4*, 194. A control experiment with Fmoc-Ser^{T}-OMe indicated that exposure to 20% piperidine led to the elimination of free thymine.
(39) Carpino, L. A. *J. Am. Chem. Soc.* **1993**, *115*, 4397.
(40) (Rink amide linker = 4-(2′,4′-dimethoxyphenylaminomethyl)phenoxyacetamido) Rink, H. *Tetrahedron Lett.* **1987**, *28*, 3787.
(41) Kamber, B.; Hartmann, A.; Eisler, K.; Riniker, B.; Rink, H.; Sieber, P.; Rittel, W. *Helv. Chim. Acta* **1980**, *63*, 899.
(42) Freier, S. M.; Burger, B. J.; Alkema, D.; Neilson, T.; Turner, D. H. *Biochemistry* **1983**, *22*, 6198.

Table 1. UV Melting Data for αPNA−DNA Complexes

Entry	αPNA-DNA Complex	T_m (°C)
1	Ac-T T T T T (b2) 5′-d(A_n-A A A A A-A_{5-n})-3′ n =10	17
2	Ac-C C C C C (b2) 5′-d(TA_3-G G G G G-A_3T)-3′	54
3	Ac-C C C C C (b1) 5′-d(TA_3-G G G G G-A_3T)-3′	34
4	Ac-C C T C C (b2) 5′-d(A_3-G G A G G-A_3)-3′	49
5	Ac-C C T C C (b2) 5′-d(TA_3-G G G G G-A_3T)-3′	38
6	Ac-C C C C C (b2) 5′-d(-G G G G G-)-3′	35

Table 2. UV Melting Data for αPNA-Dimer-d$(A)_{10}$ Complexes

Entry	αPNA-Dimer ($N \rightarrow C$)	T_m (°C)
1	S–T T T T T (b1) S–T T T T T (b1)	39
2	(b1′) T T T T T–S (b1′) T T T T T–S	51
3	S–T T T T T (b2) S–T T T T T (b2)	46,54
4	(b2′) T T T T T–S (b2′) T T T T T–S	46,57

Possible binding models:

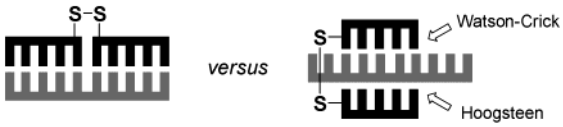

(head-to-head) dimers (Table 2, entries 1 and 2) indicating a strong orientational preference for these complexes.

Even though the stability of the resulting αPNA−DNA complexes for b1 was quite high (relative to that expected for the corresponding DNA−DNA duplex) as evident from these data, the rate of association between b1 (or b1′) αPNA and DNA was slow. We hypothesized that, at neutral pH, the Asp and Glu residues in b1 (or b1′) αPNA were negatively charged, and may have unfavorable electrostatic interactions with the negatively charged phosphate backbone of DNA, introducing a kinetic barrier to the process of association with DNA.

A new backbone was designed based on the simple logic of replacing the negatively charged Asp and Glu residues in b1 with Ala and positively charged Lys residues, respectively. Additional Lys residues were incorporated at Ala4 and Gly20, and the Aib residue was replaced by Ala. Finally, the Gly1 and Lys2 residues were interchanged in order to avoid proximal Lys residues. The resulting backbone 2 αPNAs have a net charge of +6 at neutral pH (sequence: Ac-Cys^{Acm}-Lys-Ser^{B}-Ala-Ala-Lys-Ser^{B}-Ala-Ala-Lys-Ser^{B}-Ala-Ala-Lys-Ser^{B}-Gly-Lys-NH_2; represented as BBBBB(b2), where B is a generic nucleobase).

This change brings about a remarkable enhancement in the kinetic and thermodynamic aspects of the complex formation. Compared to the CCCCC(b1)-d($TA_3G_5A_3T$) complex (T_m = 34 °C), a ΔT_m of +20 °C was observed for CCCCC(b2)-d($TA_3G_5A_3T$) (Table 1, entry 2) in TE buffer (10 mM Tris-HCl, 1 mM EDTA, pH 7) with no hysteresis observed between the heating and cooling UV melting curve. Recalling that no binding was observed between TTTTT(b1) and d(A_{10}), a T_m of 17 °C was now observed for TTTTT(b2)-d(A_{10}) (Table 2, entry 1). Binding affinity is proportional to the number of C·G versus T·A base pairs in the complex (Table 1, compare entries 1, 2, and 4). With one mismatch, a ΔT_m of −16 °C was observed for CCTCC(b2)-d($TA_3G_5A_3T$) (Table 1, entry 5). Once again, the incorporation of dangling bases at the 5′ and 3′ ends of the DNA increases the T_m of αPNA and DNA complex. Compared to CCCCC(b2)-d($AT_3G_5T_3A$), greater hysteresis, lower hyperchromicity and a lower melting temperature (T_m, 35 °C, ΔT_m −14 °C) was observed for the complex formation between CCCCC(b2) and d(G_5) (Table 1, entry 6). Both b2 (tail-to-tail) and b2′ (head-to-head) TTTTT dimers and d(A_{10}) complexes showed two-step melting (Table 2, entries 3 and 4) with nearly identical T_m values. Detailed interpretation of the two-state binding observed between homothymine αPNA-dimers and ssDNA is complicated by the fact that both duplex and triplex formation (with 1:1 or 2:1 αPNA/ssDNA binding stoichiometries) is possible.

To see whether ionic interactions between positively charged peptide backbone of b2 αPNA and negatively charged phosphate backbone of ssDNA were contributing to the binding of αPNA and ssDNA, an "abasic" peptide (Ac-Cys^{Acm}-Lys-(Ser-Ala-Ala-Lys)$_4$-Ser-Gly-Lys-NH_2) with unmodified Ser residues was also studied. No cooperative binding to d($TA_3G_5A_3T$) was observed in the UV melting curve with this abasic peptide. This indicated that the cooperative melting between αPNA and DNA was not merely a reflection of nonspecific ionic interactions.

To probe the orientational preference of αPNA binding to DNA, b2 αPNA having asymmetrical sequence (CTCCT) was synthesized and its interaction with d($A_3GAGGAA_3$) and d($A_3AGGAGA_3$) was studied. The sequence of the DNA was designed to allow only one complex to form Watson−Crick base pairs. UV melting experiments showed that the parallel orientation is more favorable than antiparallel orientation. The parallel (N-terminus of αPNA adjacent to the 5′-end of DNA or N/5′) complex has a higher melting temperature (T_m = 37 °C) and reforms during the cooling cycle more quickly than the antiparallel (N/3′) complex (T_m = 32 °C). On the UV melting experiment time scale, no reassociation was observed in the case of the antiparallel complex.

Finally, the effect of ionic strength on b2 αPNA binding to DNA was probed. Added salt can affect the properties of biological macromolecules, leading to modulation of their stability, solubility, and biological activity.[43] Increasing the ionic strength has a stabilizing effect on DNA−DNA duplexes and a destabilizing effect on Nielsen's PNA−DNA duplexes.[44] For b2 αPNA and DNA binding, the αPNA and DNA are stabilized in part by the ionic interactions (formation of ion pairs) and the concomitant release of low molecular-weight ions ($CF_3COO^-Na^+$)

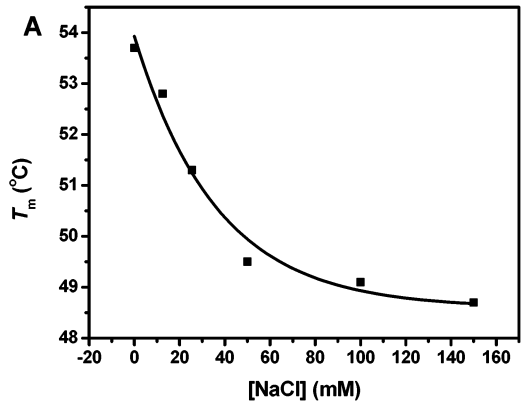

Figure 4. Effect of ionic strength (0−150 mM NaCl in 10 mM Tris-HCl, 1 mM EDTA, pH 7.0) on the T_m of CCCCC(b2)-d(*TA*$_3$G$_5$*A*$_3$*T*). Single strand concentration = 5 μM. Samples incubated overnight at 4 °C.

that were previously associated with the charged groups on the biopolymer. Because ions are released in these biopolymer charge neutralization reactions, the equilibrium shifts to favor the complex formation when the salt concentration is reduced.[45] Figure 4 shows the effect of the NaCl concentration on the T_m of a b2 αPNA−DNA complex. As the salt concentration increased, the T_m decreased. Experimentally, after 100 mM NaCl, additional salt did not affect the stability of the complex very much. A linear plot of T_m versus ln[NaCl] (not shown) was observed which may allow the theoretical calculation of T_m of αPNA−DNA at any salt concentration. The T_m of CCCCC(b2)-d(TA$_3$G$_5$A$_3$T) drops to 49 °C when the experiment is performed under simulated physiological salt concentration (150 mM NaCl). This still represents a remarkably strong binding interaction when compared to the corresponding DNA−DNA duplex, d(C$_5$)-d(TA$_3$G$_5$A$_3$T), which has a T_m of 19 °C under the same conditions.

Collectively, these thermal denaturation studies demonstrated that αPNAs bind to complementary DNA targets with high affinity and in a sequence-specific manner, consistent with our proposed base-pairing model.

3b. Gel Electrophoresis Studies on αPNA−ssDNA Complexes. Standard nondenaturing polyacrylamide gel electrophoresis (PAGE) was performed on αPNA−ssDNA complexes.[46] Only b2 αPNAs were studied due to their higher affinity toward ssDNA and their faster complexation rate compared with b1 αPNAs. b2 αPNA has six lysine residues, and the free amino groups of these lysines will be protonated under the experimental conditions; consequently, the αPNA will migrate toward the cathode during electrophoresis. The lengths of the DNA sequences were accordingly chosen to ensure that the complexes remained negatively charged and migrated toward the anode. The detection of any new species that migrates more slowly than the uncomplexed DNA would be taken as direct evidence for αPNA−ssDNA complex formation.

For the complex between CCTCC(b2) and d(*A*$_3$GGAGG*A*$_3$), a single, new, and slower-migrating species corresponding to CCTCC(b2)-d(*A*$_3$GGAGG*A*$_3$) was detected (Figure 5A). The intensity of the unbound DNA d(*A*$_3$GGAGG*A*$_3$) band steadily decreased with increased αPNA and disappeared completely at a αPNA/DNA ratio of 1.5. Triplex formation is precluded on the grounds that the resultant ternary complex would have a net positive charge and therefore be expected to migrate toward the negative electrode. Quantitative analysis of this gel (see ref 46) allowed us to determine a dissociation constant K_d of ∼ 0.2 μM (at 278 K) for this complex.

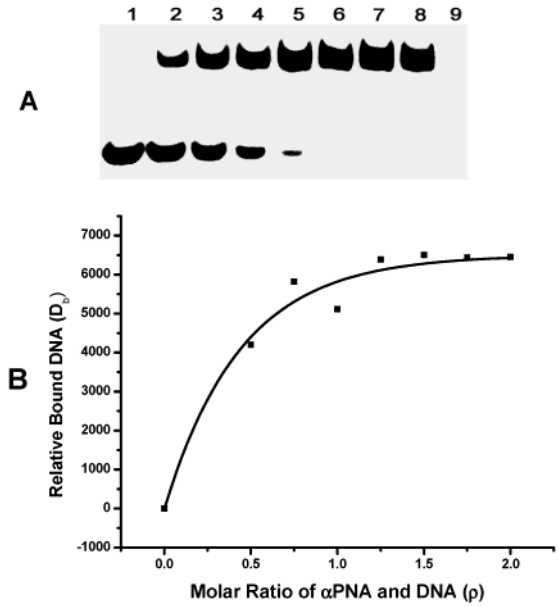

Figure 5. Nondenaturing PAGE analysis of CCTCC(b2) and d(*A*$_3$GG-AGG*A*$_3$) complex formation. The ratios of CCTCC(b2) to d(*A*$_3$GGAGG*A*$_3$) for lanes 1−8 are 0/1, 1/2, 3/4, 1/1, 5/4, 3/2, 7/4, and 2/1. Lane 9 represents only CCTCC(b2). (B) The mole ratio of αPNA and DNA (*X*-axis) is plotted vs the band intensity of the bound DNA (*Y*-axis). The titration curve shows the extent of complex formation. A K_d of ∼ 0.2 μM was derived from the data.

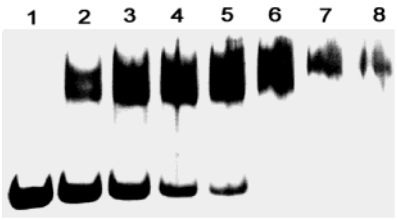

Figure 6. Nondenaturing PAGE analysis of TTTTT(b2)-dimer and d(*C*$_3$*T*-*(TC*$_2$*)*$_2$A$_{10}$*C(TC*$_2$*)*$_3$*)* complexes formation. The ratios of TTTTT(b2)-dimer to d(*C*$_3$*T(TC*$_2$*)*$_2$A$_{10}$*C(TC*$_2$*)*$_3$*)* for lanes 1−8 are 0/1, 1/2, 1/1, 3/2, 2/1, 5/2, 3/1, and 4/1.

The analogous gel shift experiment with TTTTT(b2)-dimer (net charge +12) and d(*C*$_3$*T(TC*$_2$*)*$_2$A$_{10}$*C(TC*$_2$*)*$_3$*)* (net charge −29) appeared to produce an additional slower-moving species at the expense of the initially formed complex (Figure 6). This result is consistent with the formation of binary 1:1 and ternary 2:1 complexes (recall the two-step melting of this complex in Table 2). It was not possible to distinguish between a tandem duplex or triplex structure for the 2:1 complex.

(43) Von Hippel, P. H.; Schleich, T. Effects of Neutral Salts on the Structure and Conformational Stability of Macromolecules in Solution. In *Structure and Stability of Biological Macromolecules*; Timasheff, S. N., Fasman, G. D., Eds.; Biological Macromolecules: Vol. 2; M. Dekker Inc.: New York, 1969; p 417.
(44) Tomac, S.; Sarkar, M.; Ratilainen, T.; Wittung, P.; Nielsen, P. E.; Nordén, B.; Gräslund, A. *J. Am. Chem. Soc.* **1996**, *118*, 5544.
(45) (a) Record, M. T.; Anderson, C. F.; Lohman, T. M. *Q. Rev. Biophys. II* **1978**, *2*, 103. (b) Manning, G. S. *Ibid*., 179.
(46) (a) Taylor, J. D.; Ackroyd, A. J.; Halford, S. E. The Gel Shift Assay for the Analysis of DNA-Protein Interactions. In *DNA-Protein Interactions: Principles and Protocols*; Kneale, G. G., Ed.; Methods in Molecular Biology, Vol. 30; Humana Press Inc.: Totowa, NJ, 1994; p 263. (b) Lane D.; Prentki, P.; Chandler, M. *Microbiol. Rev.* **1992**, *56*, 509.

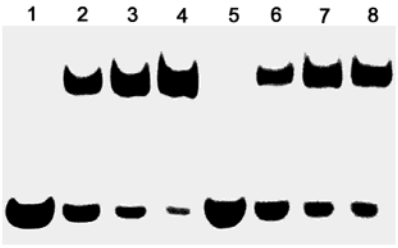

Figure 7. Nondenaturing PAGE analysis of CTCCT(b2) and d(A_3GAGGAA_3) (lanes 1−4), CTCCT(b2) and d(A_3AGGAGA_3) (lanes 5−8) complexes formation. The ratios of CTCCT(b2) to DNA for lanes 1−4 as well as 5−8 are 0/1, 1/1, 2/3, and 4/7.

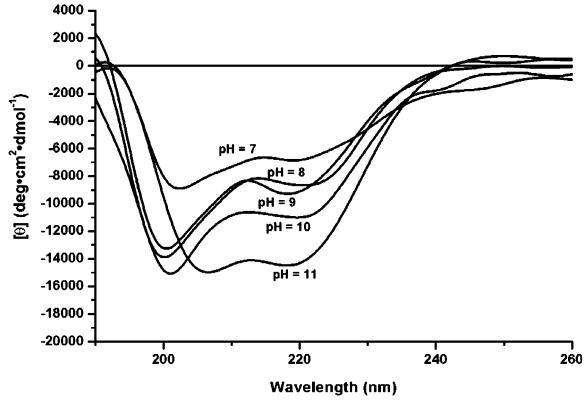

Figure 8. CD Spectra of b2 αPNA (CCTCC) obtained at different pH. Concentration: 6 μM in 17 mM phosphate buffer at 25 °C.

Similar PAGE experiments on CTCCT(b2) + d(A_3GAGGAA_3) and CTCCT(b2) + d(A_3AGGAGA_3) also confirmed that the parallel (N/5′) orientation resulted in stronger binding (Figure 7). At a particular αPNA/DNA ratio, more parallel complex was formed compared to its antiparallel counterpart. Again, no binding was observed between the "abasic" peptide Ac-Cys^{Acm}-Lys-(Ser-Ala$_2$-Lys)$_4$-Ser-Gly-Lys-NH_2) and d($TA_3G_5A_3T$), underscoring the role that nucleobases play in αPNA molecular recognition.

3c. CD Studies on αPNA−ssDNA Complexes. Circular dichroism (CD) spectroscopy has been used extensively to study peptide conformation.[47] Since αPNA has a chiral peptide backbone, the αPNA backbone itself is expected to have optical properties similar to normal peptides. We first studied the tail-to-tail TTTTT(b1)-dimer. The CD spectra were acquired at various temperatures (Supporting Information). The double minima at 220 and 206 nm as well as the maximum at 193 nm are characteristic of an α-helix.[48] With increasing of temperature, the intensity of the minimum at 200 nm decreased indicating a transition from α-helix to random structure. An isodichroic point nearly at 202 nm was suggestive of a temperature-dependent α-helix to random coil transition.[49] The helical content at 20 °C in water was estimated to be 26%. Thus, we concluded that b1 αPNA dimers are indeed α-helical in solution.

A similar pattern was noticed for b2 αPNA CCTCC(b2). At neutral pH, CCTCC(b2) is partially helical. An interesting phenomenon was revealed during the pH titration of this αPNA (Figure 8). The helicity of the backbone 2 αPNA increases with the pH. It is highly likely that as more lysines become

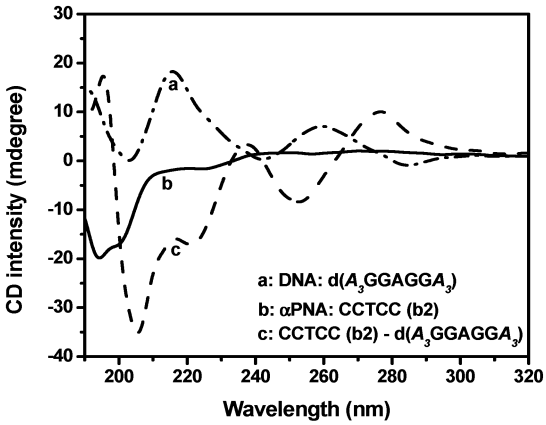

Figure 9. CD spectra of ssDNA (a), αPNA (b), and αPNA−ssDNA complex (c). Final single-stranded oligomer concentration was 6 μM in HPLC grade H_2O (pH 5.6). Spectra were recorded at 5 °C.

deprotonated with the incremental changes in pH (the pK_a of the lysine ϵ-NH_3^+ in Ala-Lys oligopeptides is approximately 11.5 in 10 mM NaCl at 0 °C),[50] the charge-repulsion between the neighboring lysine residues decreases, as a result of which the α-helix conformation is favored. Similar behavior has been reported for poly-lysine or poly-(lysine-alanine) peptides.[51]

Conformation changes induced in peptide−nucleic acid complexes can also be detected by CD spectroscopy.[52] Although the CD spectra of peptides and nucleic acids overlap extensively, they do differ in some regions. For example, above 240 nm, DNA has strong CD bands, whereas in the 210−230 nm region, the peptide CD signal is strong and nucleic acid CD signal is weak. Aromatic and sulfur-containing side chains show a major contribution around 280 nm. We used CD spectroscopy to study αPNA−DNA interactions. Trace b in Figure 9 shows the CD spectrum of αPNA CCTCC(b2) in H_2O (pH 5.6) in the absence of DNA, which suggests an almost random conformation because of the protonated Lys amines. Upon addition of an equimolar amount of ssDNA d(A_3GGAGGA_3), the characteristic CD signatures of an α-helical peptide were observed (Figure 9, trace c). Because this is a composite spectrum, the α-helix CD is superimposed upon those of other species present in the sample. Also, we cannot rule out the possibility of coexisting 3_{10}-helix and α-helix structures, since it is not possible to distinguish between them by CD methods.[53] The maximum at 280 nm and minimum at 255 nm are suggestive of an ordered right- handed DNA helix. Since the control CD spectra of αPNA and ssDNA indicate different secondary structures than the αPNA−ssDNA complex, it appears that they are mutually acting as templates for hybridization. Analogous behavior has been noted previously in studies on DNA-binding proteins[54] and synthetic peptides that correspond to the DNA-binding region of the *E. coli* RecA protein.[55] Upon binding, DNA induces the Rec24 to adopt a highly helical conformation in which the arrangement of positive charges in Rec24 is analogous to the

(47) Fasman, G. D., Ed. *Circular Dichroism and the Conformational Analysis of Biomolecules*; Plenum Press: New York, 1996.
(48) Holzwarth, G.; Doty, P. *J. Am. Chem. Soc.* **1965**, *87*, 218.
(49) Padmanabhan, S.; Baldwin, R. L. *J. Mol. Biol.* **1991**, *219*, 135.
(50) Marqusee, S.; Baldwin, R. L. *Proc. Natl. Acad. Sci. U.S.A.* **1987**, *84*, 8898.
(51) (a) Yasui, S. C.; Keiderling, T. A. *J. Am. Chem. Soc.* **1986**, *108*, 5576. (b) Satake, I.; Yang, J. *Biopolymers* **1975**, *14*, 1841. (c) Yaron, A.; Tal, N.; Berger, A. *Biopolymers*, **1972**,*11*, 2461.
(52) Talanian, R. V.; McKnight, C. J.; Kim, P. S. *Science* **1990**, *249*, 769.
(53) Sudha, T. S.; Vijayakumar, E. K. S.; Balaram, P. *Int. J. Pept. Protein Res.* **1983**, *22*, 464.
(54) (a) Patel, L.; Abate, C.; Curran, T. *Nature* **1990**, *347*, 572. (b) Weiss, M. A.; Ellenberger, T.; Wobbe, C. R.; Lee, J. P.; Harrison, S. C.; Struhl, K. *Nature* **1990**, *347*, 575.
(55) Zlotnick, A.; Brenner, S. L.; *J. Mol. Biol.* **1988**, *209*, 447.

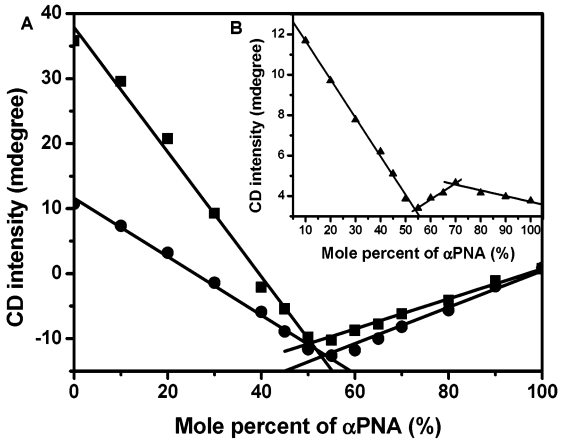

Figure 10. Job plots for CD intensities of the mixtures of DNA and αPNA. (A) CCCCC(b2)-d(*TA*$_3$G$_5$*A*$_3$*T*) (■) and CCTCC(b2)-d(*A*$_3$GGAGG*A*$_3$) (●) at 258 nm. (B) TTTTT(b2)-dimer-d(A$_{10}$) (▲) at 261 nm. Total concentration of the αPNA and DNA was 12 μM in HPLC grade H_2O (pH 5.6).

3.6 residue periodicity of hydrophobic amino acid residues in amphipathic α-helices. Taken together, these CD studies performed on complexes formed between cationic b2 αPNA and DNA not only provided support for the binding event but also for the proposed binding model. The induced conformational change of cationic b2 αPNA was coupled with specific binding between αPNA and ssDNA.

To probe for any differences between the conformations of the antiparallel and parallel complexes, CD spectra of the parallel CTCCT(b2)-d(*A*$_3$GAGGA*A*$_3$) and antiparallel CTCCT(b2)-d(*A*$_3$-AGGAG*A*$_3$) complexes were also obtained. These spectra are distinctly different, especially in the 240−280 nm regions, where the base pairs make a larger contribution in the parallel complex (Supporting Information), confirming the preference of a parallel complex for symmetrical αPNAs.

Finally, CD spectroscopy was also used to obtain accurate values for the stoichiometry of the αPNA and DNA in a complex.[56] CD spectra were recorded for mixtures of CCCCC-(b2) + d(*TA*$_3$G$_5$*A*$_3$*T*), CCTCC(b2) + d(*A*$_3$GGAGG*A*$_3$) and TTTTT(b2)-dimer + d(A$_{10}$) at different molar ratios. The CD data for monomeric modules when plotted with respect to the mole percentage of αPNA produced curves having a break point at a 1:1 molar ratio of the αPNA and DNA strands (Figure 10A). However, the TTTTT(b2)-dimer and d(A$_{10}$) showed evidence of both 1:1 and 2:1 binding stoichiometries (Figure 10B). This is in line with the UV melting data in which a two-step melting was observed (Table 2, entries 3 and 4). No minimum or maximum was observed (data not shown) for mixtures of totally mismatched αPNA CCCCC(b2) and DNA d(A$_{10}$), providing additional evidence that αPNA interacts with DNA in a sequence specific manner.

3d. NMR Studies on αPNA−ssDNA Complexes. To obtain direct evidence of specific hydrogen bonding between the nucleobases in an αPNA−ssDNA hybrid, one- and two-dimensional NMR spectra of the imino and amino protons of the nucleobases involved in base pairing were examined. Figure 11 shows the one-dimensional spectrum of αPNA alone (Figure 11A) and αPNA and ssDNA mixture (Figure 11B). Most resonance lines have different chemical shifts in the αPNA and in the αPNA−ssDNA mixture indicating complex formation. The peaks of αPNA and ssDNA in the mixture spectrum are also broader compared to the spectrum of αPNA alone. This line broadening may be due to the fact that the complex has increased molecular weight and is comparatively rigid with limited segmental mobility for the individual strands.[57]

Five exchangeable imino proton resonances are observed in the αPNA−ssDNA complex (Figure 12, the resonance of 12.83 ppm is very weak, but was resolved in the 1D-NMR at 25 °C), while no imino proton resonances are observed in the αPNA and DNA alone. These signals are relatively sharp and intense, implying that they are stabilized via hydrogen bonds through base pairing. With an increase in temperature, the complex melted and the imino proton peaks in the αPNA−ssDNA complex slowly disappeared. The chemical shift of the imino protons in DNA duplexes not only depends on the intrinsic contribution from the central residue, but also depends on the additional contributions induced by 5′- and 3′-nearest-neighbor (flanking) residues. The imino proton of thymine usually appears further downfield than the guanine imino proton.[58] Referring to the triplet case[59] (13.82 ppm for C**T**C, 12.80 ppm for A**G**G, and 12.66 ppm for G**G**A), 13.44 ppm is assigned as the thymine N^3-H peak. The signals of the NH (imino) protons of G and T move upfield as the temperature increases; G-NH (imino) moves more slowly than does T-NH (imino) due to an increasing exchange with the water solvent. This is consistent with our assignment. The two peaks with relatively high intensity (12.72, 12.52 ppm) are assigned as the G5/G7 imino protons. The remaining peaks (13.15, 12.83 ppm) are assigned to the end bases G4 and G8 (refer to Figure 13 for the numbering system of ssDNA and αPNA).

The NOESY spectrum of the complex in phosphate buffer at 5 °C also exhibits several cross-peaks involving the imino protons (Figure 13). For the A·T base pairs, there was a strong NOE correlation from the thymine imino to the H-2 of the paired adenine (7.64 ppm) and a weaker NOE correlation to the adenine N^6-H (7.81 ppm).[60] For the G·C base pairs, relatively strong cross-peaks between the guanine imino protons and the amino protons on the paired cytosine were seen except for the end bases G4/G8. For the guanine imino protons (12.52 ppm), cross-peaks between the guanine imino protons and the amino protons on the paired cytosine were seen (8.10/6.30 ppm, cross-peaks between these two amino protons are observed). For the imino proton at 12.72 ppm, cross-peaks between both N^4-H of cytosine and N^2-H of guanine were observed (7.93/6.37, 8.04/5.97; cross-peaks between 7.93/6.37 and 8.04/5.97 identify the two amino groups). The strong cross-peaks for the amino protons indicates either a slow or restricted rotation of the amino groups, which is expected if they are engaged in the base pairing. A Hoogsteen base pairing scenario can be excluded on the basis that no cross-

(56) (a) Kim, S. K.; Nielsen, P. E.; Egholm, M.; Buchardt, O.; Berg, R. H.; Norden, B. *J. Am. Chem. Soc*., **1993**, *115*, 6478. (b) Wittung, P.; Kim, S. K.; Buchardt, O.; Nielsen, P.; Norden, B. *Nucleic Acid Res.* **1994**, *22*, 5371. (c) Wittung, P.; Nielsen, P.; Norden, B. *J. Am. Chem. Soc*., **1996**, *118*, 7049. (d) Gray, D. M.; Hung, S.; Johnson, K. H. *Methods Enzymol.* **1995**, *246*, 19.

(57) Wüthrich, K. *NMR of Proteins and Nucleic Acids*; Wiley & Sons: New York, 1986.

(58) Leijon, M.; Gräslund, A.; Nielsen, P. E.; Buchardt, O.; Nordén, B.; Kristensen, S. M.; Eriksson, M. *Biochemistry* **1994**, *33*, 9820.

(59) Altona, C.; Faber, D. H.; Hoekzema, A. W. *Magnetic Reson. Chem.* **2000**, *38*, 95.

(60) Brown, S. C.; Thomson, S. A.; Veal, J. M.; Davis, D. G. *Science* **1994**, *265*, 777.

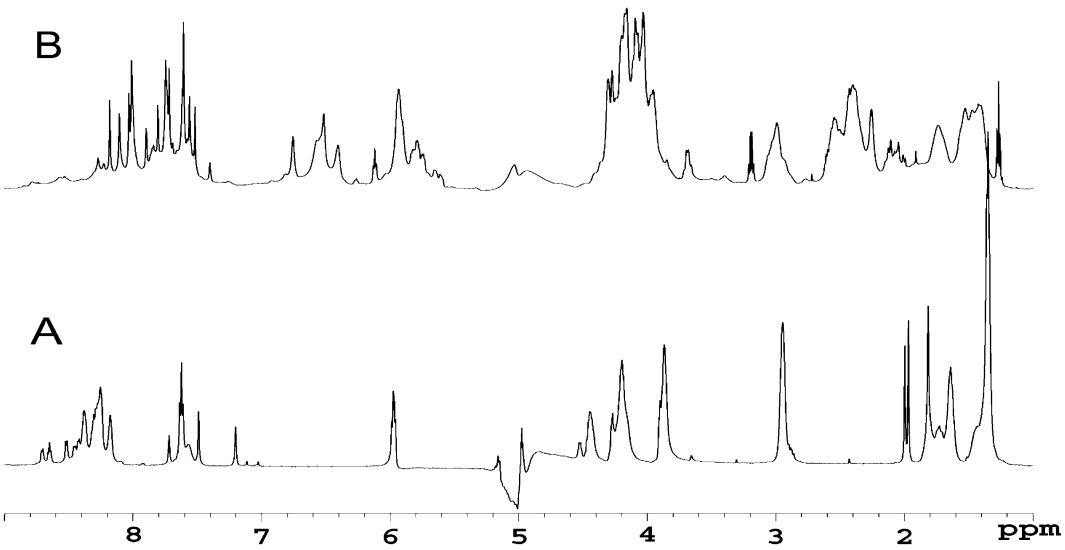

Figure 11. ^{1}H NMR spectra of αPNA CCTCC(b2) (A) and the CCTCC(b2)-d(A_3GGAGGA$_3$) (1 to 1 ratio) complex (B) recorded at 600 MHz and 5 °C.

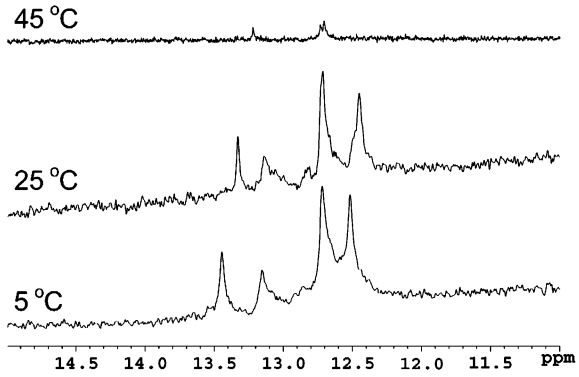

Figure 12. ^{1}H NMR spectra of the imino proton region of the d(A_3GG-AGGA_3)-CCTCC(b2) complex (1:1 ratio) at different temperatures.

peaks are observed between the thymine imino protons and the H-8 proton on the partner adenine.

In all, the data presented here clearly demonstrates that the αPNA−ssDNA complex is associated through Watson−Crick base pairs. Overlap of the ssDNA and αPNA resonances makes a detailed conformational characterization of the αPNA−ssDNA complex very challenging. For complete elucidation of the three-dimensional structure of this αPNA−ssDNA complex, information rich data using different NMR experiments should be acquired and isotopically labeled αPNA or ssDNA may be used. αPNAs having unsymmetrical amino acid sequences may allow better dispersion of the data.

Conclusions

A novel platform for nucleic acid recognition that merges the α-helix secondary structure of peptides with the codified base-pairing capability of nucleic acids has been designed. Effective syntheses of the constituent Fmoc-protected thymine, cytosine, and uracil nucleoamino acids **6**, **10**, and **13** were developed along with protocols for the solid-phase synthesis of 21mer αPNAs containing five nucleobases as well as their conversion into symmetrical disulfide-bridged αPNA dimers (containing 10 nucleobases). The binding of αPNA to ssDNA was examined by thermal denaturation, gel electrophoresis, circular dichroism, and NMR spectroscopy.

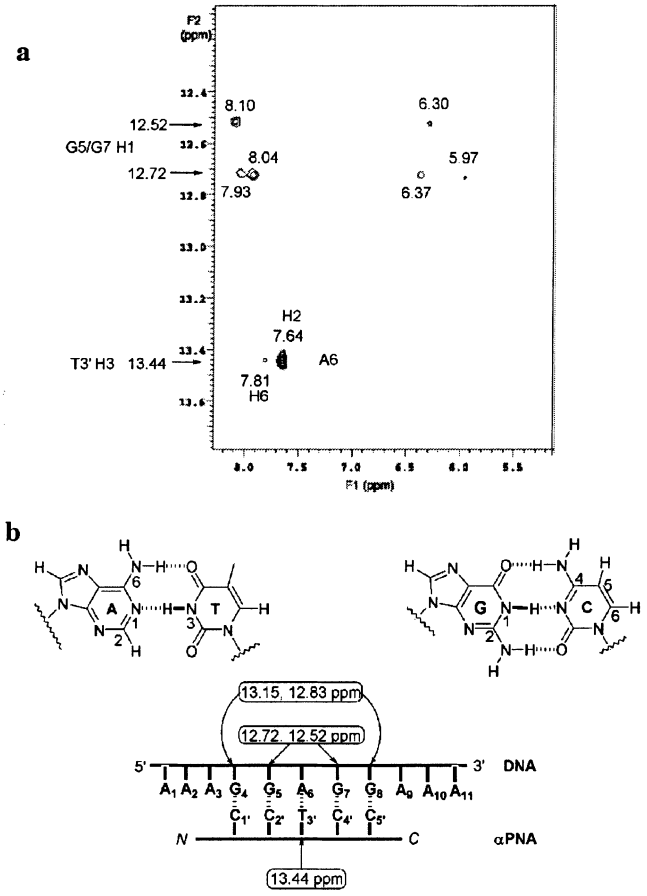

Figure 13. (a) NOESY spectrum of the imino proton region of the CCTCC-(b2)-d(A_3GGAGGA$_3$) complex (1:1 ratio) at 5 °C. (b) Diagrams showing the imino protons after hydrogen bonding and the numbering system for ssDNA and αPNA.

The following conclusions can be drawn from these data. αPNAs bind to ssDNAs in a cooperative manner with high affinity and sequence specificity. In general, b2 αPNAs bind faster and more strongly with ssDNA than do the corresponding b1 αPNAs. Parallel αPNA−DNA complexes are more stable than their antiparallel counterparts. CD studies also revealed that the hybridization event involves the folding of both species

into their helical conformations. Finally, NMR experiments provided conclusive evidence of Watson−Crick base pairing in αPNA−ssDNA hybrids.

These studies constitute the proof of principle for αPNA hypothesis and set the stage for further exploration of this novel platform for nucleic acid recognition.

Experimental Section

1. Nucleoamino Acid Synthesis. Instrumentation. All reported melting points were determined using a Mel-Temp capillary melting point apparatus and are not corrected. Optical rotations were measured using a Perkin-Elmer 241 polarimeter at either $\lambda = 589$ nm (sodium D line) or $\lambda = 578$ nm (mercury J line) at RT and were reported as follows: $[\alpha]^{T}_{D \text{ or } J}$, concentration ($c$ = g/100 mL), and solvent. NMR spectra were recorded on Varian Inova 500 or Gemini-300 NMR spectrometers and are reported in parts per million (ppm) on the δ scale relative to residual $CHCl_3$ (δ 7.25 or δ 77.0), C_6H_6 (δ 7.15), H_2O (δ 4.75), DMSO-d_6 (δ 2.49, δ 39.5), tetramethylsilane (δ 0.00), or DSS (2,2-dimethyl-2-silapentane-5-sulfonic acid, δ 0.00) for ^{1}H or ^{13}C. Proton and carbon assignments are based on COSY and HETCOR experiments. High-resolution mass spectral (HRMS) data were obtained from a KRATOS Analytical MS25RFA spectrometer and are reported in units of m/z for M^+ or the highest mass fragment derived from M^+.

Solvents and Reagents. All moisture-sensitive reactions were performed in an inert, dry atmosphere of Ar. Reagent grade solvents were used for chromatography and extraction. The following solvents and reagents were purified beyond reagent grade: Tetrahydrofuran (THF) was distilled under Ar or N_2 from a purple solution of sodium−benzophenone ketyl. Dichloromethane (DCM), 1,2-dichloroethane, and CH_3CN were distilled over CaH_2 (0−1 mm grain size) under an Ar atmosphere. Dimethyl sulfoxide (DMSO) was distilled from CaH_2 under reduced pressure and stored over 4 Å MS. 1,1,1,3,3,3-Hexamethyldisilazane (HMDS), chlorotrimethylsilane (TMSCl), thymine, cytosine, uracil, benzyl bromide, benzoyl peroxide, tetrabutylammonium iodide, 4-(dimethylamino)pyridine (DMAP), di-*tert*-butyl dicarbonate ($(Boc)_2O$), dimethyl sulfide, *N*,*O*-bis-trimethylsilylacetamide (BSA), formic acid (96% in water), trifluoroacetic acid (TFA), 1,4-cyclohexadiene, and Pd−C (10% w/w) were used as received from Aldrich.

Chromatography. Thin-layer chromatography (TLC) was performed using either Merck silica gel 60 F-254 plates or JT-Baker Si 250F plates (0.25 mm thickness). The plates were visualized first with UV illumination followed by charring with 0.3% (w/v) ninhydrin solution in (97:3) EtOH−AcOH. Flash chromatography was performed using silica gel (230−400 mesh).

HMBC/HMQC NMR Experiments. These experiments were performed at 500 MHz (Varian, Inova 500) at ambient temperature using 70−100 mg of sample in 750 μL of D_2O as solvent. HMQC parameters: sw (spectral width) = 6000 Hz, np (number of points) = 600 and nt (number of transients) = 8. HMBC parameters: sw = 6000 Hz, τ_{mb} (reciprocal of multiple bond H−C coupling constant) = 0.05 s and nt = 16.

Fmoc-Ser-OBn (2). Dry DMSO (3 mL) was added to a 25 mL Ar-flushed flask containing **1** (0.481 g, 1.47 mmol), $KHCO_3$ (0.221 g, 2.20 mmol), and tetrabutylammonium iodide (0.0543 g, 0.147 mmol). The resulting white suspension was stirred magnetically at room temperature for 10 min to obtain a homogeneous solution. To this solution was added benzyl bromide (0.524 mL, 4.40 mmol), and the colorless reaction mixture was stirred for 8 h at room temperature. TLC analysis of the resulting brownish-yellow solution showed the formation of a single product and presence of trace amount of starting material. The reaction was quenched by addition of 25 mL of water, and the DMSO−water layer was extracted with EtOAc (3 × 75 mL). The combined organic layers were washed, first with saturated aq $NaHCO_3$ (3 × 50 mL) to remove **1** completely (analyzed by TLC), then with saturated aq $Na_2S_2O_3$ (2 × 50 mL), and finally with brine (1 × 50 mL). The organic layer was dried (Na_2SO_4) and concentrated by rotary evaporation, and the residual EtOAc was removed under vacuum to give a yellow oil. The oil was cooled to −78 °C (dry ice/acetone) and triturated with hexanes. The yellow solid thus obtained was transferred to a Büchner funnel (filter paper) and washed with hexanes under suction until a white solid was obtained (0.563 g, 92% yield). mp 96−97 °C; R_f = 0.20, 3:7 EtOAc−hexanes; $[\alpha]^{26}_D = +0.63°$ (*c* 4.45, DCM); ^{1}H NMR (300 MHz, $CDCl_3$) δ 7.77 (d, J = 7.6 Hz, 2H), 7.60 (d, J = 7.5 Hz, 2H), 7.26−7.43 (m, 9H), 5.75 (dd, J_1 = 7.0 Hz, J_2 = 1.1 Hz, NH), 5.23 (s, 2H, CH_2Ph), 4.20−4.50 (m, 3H, H-2 + 2 × H-10′), 4.22 (t, J = 6.7 Hz, 1H, H-9′), 4.07 (dd, J_1 = 16.5 Hz, J_2 = 1.8 Hz, 2H, CH_2OH), 2.15 (broad s, 1H, OH). ^{13}C NMR (75.4 MHz, $CDCl_3$) δ 170.4, 156.2, 143.7, 143.6, 141.2, 135.0, 128.6, 128.4, 128.1, 127.0, 125.0, 119.9, 67.4 (*C*H_2Ph), 67.2 (C-10′), 63.1 (C-3), 56.1 (C-2), 47.0 (C-9′). HRMS (EI) m/z, calcd for $C_{25}H_{23}NO_5$ [M^+] 417.1576, obsd 417.1574.

Fmoc-Ser(MTM)-OBn (3). A three-neck 250 mL round-bottom flask equipped with a magnetic stir bar and solid addition assembly containing benzoyl peroxide (19.6 g, 0.081mol), was charged with **2** (9.66 g, 0.0232 mol). After flushing the system with Ar, 130 mL of dry CH_3CN was added with stirring and the mixture was cooled to 0 °C (ice−water). To the cold solution was added Me_2S (11.9 mL, 0.162 mol)), followed by solid benzoyl peroxide over a period of 30 min from the solid addition assembly. The reaction was complete after stirring for additional 1 h at 0 °C (a second development, after complete drying, of a 5.5 cm TLC plate with 3:7 EtOAc−hexanes clearly demonstrated the absence of starting material). The reaction was then quenched with 100 mL of water and extracted with ether (3 × 250 mL). The combined organic layer was washed with saturated aq $NaHCO_3$ (3 × 75 mL) followed by 1 N aq HCl (3 × 75 mL) and brine (1 × 75 mL), dried (Na_2SO_4), and concentrated by rotary evaporation to give a white solid. The solid was purified by flash chromatography on silica gel (6.5 × 17.5 cm bed, column packed with 1:9 EtOAc−hexanes, sample loaded onto the column with $CHCl_3$; gradient elution, 1000 mL of 1:9 EtOAc−hexanes then 1000 mL of 1:4 EtOAc−hexanes followed by 500 mL of 3:7 EtOAc−hexanes) to afford 7.21 g of pure product and some fractions containing slightly impure product which were combined and rechromatographed (4 × 20 cm bed, column packed with 1:9 EtOAc−hexanes; sample loaded with $CHCl_3$; eluted with 600 mL of 3:7 EtOAc−hexanes) to afford another 2.58 g (89% yield) of pure **3**. mp 79−80 °C; R_f = 0.71, 3:2 hexanes−EtOAc; $[\alpha]^{25}_D = -8.08°$ (*c* 1.36, DCM); ^{1}H NMR (300 MHz, $CDCl_3$) δ 7.75 (d, J = 7.5 Hz, 2H), 7.60 (d, J = 7.5 Hz, 2H), 7.24−7.42 (m, 9H), 5.70 (d, J = 8.7 Hz, NH), 5.34 (dd, J_1 = 19.5 Hz, J_2 = 12.3 Hz, 2H, CH_2Ph), 4.33−4.64 (m, 5H, H-2 + 2 × H-10′ + 2 × H-3), 4.22 (t, J = 7.0 Hz, 1H, H-9′), 4.04 (dd, J_1 = 9.6 Hz, J_2 = 3.0 Hz, H-3a), 3.76 (dd, J_1 = 9.3 Hz, J_2 = 3.0 Hz, H-3b), 2.00 (s, 3H, SCH_3); ^{13}C NMR (75.4 MHz, $CDCl_3$) δ 170.0, 155.9, 143.9, 143.7, 141.2, 141.2, 135.2, 128.6, 128.2, 127.7, 127.0, 125.1, 125.1, 119.9, 75.6 (*C*H_2SMe), 67.8 (C-3), 67.4 (*C*H_2Ph), 67.2 (C-10′), 54.2 (C-2), 47.1 (C-9), 13.7 (*SC*H_3). HRMS (EI) m/z, calcd for $C_{27}H_{27}NO_5S$ [M^+] 477.1609, obsd 477.1619.

Fmoc-Ser^T-OBn (5) A flask containing 1.48 g of crushed 3 Å MS was flame dried under vacuum, flushed with argon, and then cooled to room temperature. A solution of **3** (1.48 g, 3.11 mmol in 6.0 mL dry THF) was transferred to the flask, followed by the addition of a solution of **4** (4.2 g, 15.5 mmol, in 6.4 mL of dry THF) and a solution of I_2 (1.18 g, 4.67 mmol, in 6.0 mL of dry THF). The reaction mixture was stirred at room temperature under an Ar atmosphere for 48 h whereupon TLC analysis showed only the presence of product and some unconverted **3**. The reaction mixture was poured into a 5% (w/v) aqueous solution of Na_2SO_3 (100 mL) and stirred vigorously whereupon a white precipitate formed. The mixture was suction filtered, and the solid residue in the Büchner funnel was washed with THF until the washing was free of product (TLC analysis). Excess THF was evaporated from the filtrate by rotary evaporation, and the aqueous emulsion so formed was extracted with $CHCl_3$ (3 × 100 mL). The

combined $CHCl_3$ layers were washed with brine (2 × 100 mL), dried over Na_2SO_4, and concentrated by rotary evaporation to give a white solid. The solid was purified by flash chromatography using silica gel (4 × 17.5 cm bed, column packed with 1:9 EtOAc−hexanes) The sample was loaded onto the column with $CHCl_3$, and 20 mL of additional $CHCl_3$ was used to embed the sample onto the silica. This step is necessary to avoid precipitation of solid on the top of the column upon addition of eluting solvent. The column was eluted initially with 1:1 EtOAc−hexanes (200 mL) to recover 0.539 g of the starting material and then with 7:3 EtOAc−hexanes to give 1.036 g of pure **5** (60% yield; 95% based on recovered **3**): mp 69 °C; R_f = 0.46, 1:4 hexanes−EtOAc; $[\alpha]^{26}_D = +2.20°$ (*c* 1.45, DCM); ^{1}H NMR (300 MHz, $CDCl_3$) δ 8.66 (s, 1H, NH), 7.77 (d, *J* = 7.2 Hz, 2H), 7.60 (d, *J* = 7.5 Hz, 2H), 7.27−7.43 (m, 9H), 6.97 (s, 1H, H-6′), 5.72 (d, *J* = 8.7 Hz, NH), 5.20 (AB quartet, J_{AB} = 12.3 Hz, 2H, 2 × H-1‴), 5.03 (s, 2H, CH_2Ph), 4.60 (m, 1H, H-2), 4.33−4.48 (m, 2H, 2 × H-10″), 4.22 (t, *J* = 6.6 Hz, 1H, H-9″), 4.04 (dd, J_1 = 10.2 Hz, J_2 = 3.3 Hz, H-3a), 3.88 (dd, J_1 = 9.9 Hz, J_2 = 3.3 Hz, H-3b), 1.88 (s, 3H, 5′-Me); ^{13}C NMR (75.4 MHz, $CDCl_3$) δ 169.7, 163.7, 155.9, 151.0, 143.7, 141.3, 138.7, 128.7, 128.7, 128.3, 127.80, 127.1, 125.2, 125.1, 76.8 (*C*H_2Ph), 69.6 (C-3), 67.6 (C-1‴), 67.3 (C-10″), 54.3 (C-2), 47.1 (C-9″), 12.3 (5′-*C*H_3). HRMS (FAB, CsI/NaI/glycerol matrix) *m*/*z*, calcd for $C_{31}H_{29}N_3O_7$ [MCs$^+$] 688.1060, obsd 688.1046.

Fmoc-Ser^T-OH (6). Pd−C catalyst (10%, 500 mg) was added as a slurry in THF to a solution of **5** (1.52 g, 2.73 mmol) in 100 mL of (1:1) THF−MeOH and stirred while H_2 was bubbled through the reaction mixture at a moderate rate. A solution of 1:1 THF−MeOH was periodically added to the reaction mixture to replenish the evaporating solvent. After 45 min, TLC examination showed clean conversion of starting material to product. The H_2 flow was then replaced by Ar for another 10 min, at which point the reaction mixture was filtered and washed (THF) through a pad of Celite until the washing was free of product (TLC analysis). Upon concentration of the filtrate a sticky foam was obtained, from which the residual MeOH was removed by coevaporation with $CHCl_3$ (3 mL × 3) to afford 1.280 g (quantitative yield) of a white solid. mp 80 °C (decomposed); R_f = 0.20, 90:8:2 $CHCl_3$−CH_3OH−AcOH; $[\alpha]^{23}_J = +34.1°$ (*c* 1.11, $CHCl_3$); ^{1}H NMR (300 MHz, $CDCl_3$) δ 10.22 (s, 1H, NH), 9.2 (broad singlet, 1H, COOH), 7.73 (d, *J* = 7.1 Hz, 2H), 7.60 (t, *J* = 7.2 Hz, 2H), 7.37 (t, *J* = 7.8 Hz, 2H), 7.28 (t, *J* = 7.2 Hz, 2H), 7.05 (s, 1H, H-6′), 6.11 (d, 7.8 Hz, NH), 5.03 (AB quartet, J_{AB} = 9.9 Hz, 2H, 2 × H-1‴), 4.55 (m, 1H, H-2), 4.33−4.47 (m, 2H, 2 × H-10″), 4.19 (t, 1H, *J* = 7.2 Hz, H-9″), 4.04 (broad doublet, *J* = 7.8 Hz, 1H, H-3a), 3.92 (broad doublet, *J* = 8.1 Hz, 1H, H-3b), 1.82 (s, 3H, 5′-Me); ^{13}C NMR (75.4 MHz, $CDCl_3$) δ 165.0, 156.4, 151.8, 143.9, 143.8, 141.2, 140.0, 127.8, 127.1, 125.3, 125.2, 120.0, 111.5, 77.2, 69.5 (C-3), 67.2 (C-10″), 54.6 (C-2), 47.1 (C-9″), 12.1 (5′-Me); HRMS (FAB, CsI/NaI/glycerol matrix) *m*/*z*, calcd for $C_{24}H_{23}N_3O_7$ [MCs$^+$] 598.0590, obsd 598.0620, calcd [MNa$^+$] 488.1433, obsd 488.1436.

***N*^{4}-Boc-Cytosine (7).** Cytosine (14.7 g, 0.132 mol) and DMAP (0.808 g, 6.61 mmol) were added to a dry 500 mL one-necked round-bottom flask, equipped with a magnetic stir bar and a rubber septum, which was vented through an oil bubbler. The apparatus was flushed with Ar, and 240 mL of dry DMSO was added. The resulting white suspension was stirred at room temperature for 10 min, and then $(Boc)_2O$ (38.0 mL, 0.165 mmol) was added, when the mixture became homogeneous. The light yellow solution was stirred for an additional 24 h at room temperature, during which time some white solid precipitated. Completion of the reaction was confirmed by analysis of ^{1}H NMR (1 mL of the reaction mixture was transferred by a syringe to a flask containing 10 mL water. The white precipitate formed was filtered and washed with 10 mL each of water, MeOH, EtOAc, and hexanes consecutively. After drying under vacuum, the ^{1}H NMR spectrum of this white solid was obtained). The reaction mixture was transferred to a 2 L flask containing 1 L of water. The resulting suspension was stirred vigorously for 30 min and then suction filtered. The yellow solid was washed first with 1 L of water and then with 500 mL each of EtOAc and hexanes successively to afford 14.97 g (54% yield) of pure product as a white solid, which was dried in a P_2O_5 desiccator. mp 270 °C (decomposed); R_f = 0.81, 4:1:1 *t*-BuOH−AcOH−H_2O; ^{1}H NMR (300 MHz, DMSO-d_6) δ 7.73 (d, *J* = 7.1 Hz, 1H, H-6), 6.87 (d, *J* = 7.1 Hz, 1H, H-5), 1.44 (s, 9H, (CH_3)$_3$CO). ^{13}C NMR (75.4 MHz, DMSO-d_6) δ 173.7 (C-6), 162.8 (C-2), 154.5, 146.3, 93.5 (C-5), 80.7 ((CH$_3$)$_3$*C*O), 27.8 ((*C*H$_3$)$_3$CO); HRMS (EI) *m*/*z*, calcd for $C_9H_{13}N_3O_3$ M$^+$ 211.0957, obsd 211.0950.

***N*^{4}-Boc-Cytosine·TMS (8).** After flushing a dry 250 mL, one-necked, round-bottom flask, equipped with a magnetic stirring bar and a rubber septum containing *N*^{4}-Boc cytosine (6.06 g, 28.7 mmol) with Ar, CH_3CN (121 mL) and BSA (7.10 mL, 28.7 mmol) were added. The resulting suspension was stirred at room temperature for 2 h, and more BSA (3.55 mL, 14.4 mmol) was added. The reaction mixture became a clear light-yellow solution after 15 min. Stirring was continued at room temperature for another 2 h under Ar atmosphere, and the contents was transferred to a flame-dried short path distillation assembly (flushed with Ar). The CH_3CN was first distilled under reduced pressure at room temperature, and then the residual liquid was heated at 40−50 °C under reduced pressure (1−2 mmHg) for 12 h to afford a white solid. The solid (8.13 g, 100%) in the flask was used directly in the next reaction without further purification. ^{1}H NMR (300 MHz, C_6D_6, distilled from Na) δ 8.54 (s, NH), 8.3 (d, *J* = 11.3 Hz, 1H, H-6) 7.67 (d, *J* = 11.40 Hz, 1H, H-5), 1.30 (s, 9H, (CH$_3$)$_3$CO), 0.34 (s, 9H, (CH$_3$)$_3$-SiO).

Fmoc-Ser$^{C(Boc)}$-OBn (9). A flask containing 0.63 g of crushed 3 Å MS was flame dried under vacuum, flushed with Ar, and then cooled to room temperature. A solution of **3** (0.628 g, 1.32 mmol in 3 mL dry THF, 0.44 M) was transferred to the flask, followed by the addition of a solution of **8** (0.701 g, 1.97 mmol in 1.4 mL of dry THF, 1.0 M) and a solution of iodine (0.334 g, 1.32 mmol in 4 mL of dry THF). The reaction mixture was stirred at room temperature under Ar atmosphere for 48 h whereupon TLC analysis showed only the presence of the product and unconverted **3**. The reaction mixture was worked up similarly as in the case of compound **5** to give a white solid. The solid was purified by flash chromatography on silica gel (5.5 × 12 cm bed, column packed with 1:9 EtOAc−hexanes). The sample was loaded onto the column with a minimum amount of $CHCl_3$, and 5 mL of additional $CHCl_3$ was used to embed the sample onto the silica gel. The column was eluted first with 1:1 EtOAc−hexanes to afford 0.112 g of starting material **3**, and then with 5:2:3 EtOAc-THF−hexanes to afford 0.402 g of pure **9** (46% yield, 96% based on recovered starting material). mp 177−178 °C; R_f = 0.40, 5:2:3 EtOAc−THF−hexanes; $[\alpha]^{25}_J = +1.17°$ (*c* 1.96, DCM); ^{1}H NMR (300 MHz, $CDCl_3$) δ 7.76 (d, *J* = 7.4 Hz, 2H), 7.60 (d, *J* = 7.1 Hz, 2H), 7.26−7.43 (m, 10H), 7.15 (d, *J* = 7.4 Hz, 1H, H-5′), 5.76 (d, *J* = 8.5 Hz, NH), 5.60−5.62 (m, 4H, *CH*$_2$Ph, 2 × H-1‴), 4.58 (m, 1H, H-2), 4.32−4.48 (m, 2H, 2 × H-10″), 4.22 (t, *J* = 7.0 Hz, 1H, H-9″), 4.07 (dd, J_1 = 2.9 Hz, J_2 = 9.5 Hz, H-3a), 3.90 (dd, J_1 = 2.6 Hz, J_2 = 9.8 Hz, H-3b), 1.56 (s, 9H, (CH_3)$_3$CO); ^{13}C NMR (75.4 MHz, $CDCl_3$) δ 169.7, 163.0, 155.9, 155.7, 150.9, 146.6 (C-6′), 143.8, 143.7, 141.3, 135.1, 128.6, 128.5, 128.3, 127.7, 127.1, 125.1, 125.0, 119.9, 95.8 (C-5′), 83.0 ((CH$_3$)$_3$*C*O), 78.3, 69.9 (C-3) 67.5, 67.2 (C-10″) 54.3 (C-2) 47.1 (C-9″) 28.0 ((*C*H$_3$)$_3$CO); HRMS (FAB, CsI/NaI/glycerol matrix) *m*/*z*, calcd for $C_{35}H_{36}N_4O_8$ [MH]$^+$ 641.2611, obsd 641.2614.

Fmoc-Ser$^{C(Boc)}$-OH (10). Compound **9** was dissolved in minimum volume of THF (approximately 25 mL/0.5 g) by stirring, and equal volume of MeOH was added. To this solution was added a slurry of 2 equiv (by weight) of Pd−C (10%) in THF. After bubbling Ar through the reaction mixture for 5 min, 10 equiv of 1,4-cyclohexadiene was added, and the resulting mixture was stirred until completion of the reaction (30−45 min). In case of incomplete reaction, an additional 5 equiv of 1,4-cyclohexadiene drives the reaction to completion within 10 min. Filtration and washing (THF) through a Celite pad followed by rotary evaporation of the solvent gave the product in the form of

white foam in quantitative yield. mp 130 °C (formation of foam); R_f = 0.40, 4:1 $CHCl_3$−MeOH; $[\alpha]^{25}_J$ = +29.6° (*c* 0.45, DCM); ^{1}H NMR (300 MHz, DMSO-d_6) δ 10.50 (br s, 1H), 8.04 (d, *J* = 7.3 Hz, 1H, H-6′), 7.87 (d, *J* = 7.3 Hz, 2H), 7.73 (d, *J* = 7.5 H, 2H), 7.68 (d, *J* = 8.4 Hz, 1H), 7.40 (dd, J_1 = 6.9 Hz, J_2 = 7.2 Hz, 2H), 7.32 (dd, J_1 = 7.3 Hz, J_2 = 6.8 Hz, 2H), 7.08 (d, *J* = 6.9 Hz, 1H, H-5′), 6.99 (d, *J* = 7.4 Hz, NH), 6.86 (br s, 1H), 6.64 (br s, 1H), 5.21 (s, 2H, 2 × H-1‴), 4.18−4.30 (m, 4H, H-2, 2 × H-10″, H-9″), 3.80 (m, 1H, H-3a), 3.58 (m, 1 × H-3b), 1.43 (s, 9H, $(CH_3)_3CO$); ^{13}C NMR (75.4 MHz, DMSO-d_6) δ 163.6, 155.7, 155.2, 152.2, 148.7 (C-6′), 143.9, 140.7, 139.3, 127.6, 127.0, 125.2, 124.9, 120.1, 94.6 (C-5′), 81.0 ($(CH_3)_3CO$), 78.1, 69.8, 67.0, 65.6, 55.5, 46.7 (C-9″), 27.8 ($(CH_3)_3CO$). HRMS (FAB, CsI/NaI/glycerol matrix) *m*/*z*, calcd for $C_{28}H_{30}N_4O_8$ $[MCs]^+$ 683.11180, obsd 683.11146. calcd for $[(M-H)Cs_2]^+$ 815.0094, obsd 815.0093.

Fmoc-Ser^U-OBn (12) A flask containing 3.0 g of crushed 3 Å MS was flame dried under vacuum, flushed with Ar, and then cooled to room temperature. A solution of Fmoc-Ser^{MTM}-OBn (**3**, 2.97 g, 6.23 mmol in 12 mL dry THF) was transferred to the flask, followed by addition of a solution of U·2TMS **11** (3.20 g, 12.5 mmol, in 6.8 mL of dry THF) and a solution of I_2 (2.37 g, 9.35 mmol, in 18.3 mL of dry THF). The reaction mixture was stirred at room temperature under an Ar atmosphere for 12 h whereupon TLC analysis showed mainly the presence of one product and some unconverted **3**. The reaction mixture was worked up similarly as in the case of compound **5** to give a white solid. The solid was purified by flash chromatography using silica gel (4 × 20 cm bed, column packed with 1:9 EtOAC-hexanes). The sample was loaded onto the column with $CHCl_3$, and 20 mL of additional $CHCl_3$ was used to embed the sample onto the silica gel. The column was eluted initially with 4:5:1 EtOAc−hexanes−THF (1 L) to recover 2.0 g of the starting material and then with 5:3:2 EtOAc−hexanes−THF to give 0.8161 g of pure product (24% yield; 74% based on recovered starting material **3**). mp 54 °C (thawed) and 68 °C (formed glass); R_f = 0.36, 5:3:2 EtOAc−hexanes−THF; $[\alpha]^{25}_D$ = +1.3° (*c* 2.8, DCM); ^{1}H NMR (300 MHz, $CDCl_3$) δ 9.34 (s, 1H, NH), 7.75 (d, *J* = 7.3 Hz, 2H), 7.59 (d, *J* = 6.9 Hz, 2H), 7.36−7.41 (t, *J* = 7.3 Hz, 2H), 7.27−7.33 (m, 7H), 7.00 (d, *J* = 7.9 Hz, 1H, H-6′), 5.80 (d, *J* = 8.3 Hz, 1H), 5.60 (dd, J_1 = 8.4 Hz, J_2 = 1.5 Hz, NH), 5.11−5.25 (m, 2H, 2 × H-1‴), 5.01 (s, 2H, CH_2Ph), 4.58 (m, 1H, H-2), 4.33−4.46 (m, 2H, 2 × H-10″), 4.20 (t, *J* = 6.9 Hz, 1H, H-9″), 4.00 (dd, J_1 = 9.9 Hz, J_2 = 3.0 Hz, H-3a), 3.88 (dd, J_1 = 9.9 Hz, J_2 = 3.0 Hz, H-3b); ^{13}C NMR (75.4 MHz, $CDCl_3$) δ 169.2, 162.8, 155.4, 150.5, 143.3, 142.3, 140.8, 134.6, 128.4, 128.2, 128.0, 127.3, 126.6, 125.0, 124.6, 119.5, 102.9, 76.3 (*C*H_2Ph), 69.1 (C-3), 67.1 (C-1‴), 66.7 (C-10″), 53.7 (C-2), 46.6 (C-9″). HRMS (FAB, CsI/NaI/glycerol matrix) *m*/*z*, calcd for $C_{30}H_{28}N_3O_7$ $[MH]^+$ 542.1927, obsd 542.1928.

Fmoc-Ser^U-OH (13). The benzyl group was removed from **12** in a similar way as in the case of compound **9** to give product **13** as a white foam in quantitative yield. mp 110 °C (thawed) and 124 °C (formed glass); R_f = 0.27, 4:1 $CHCl_3$−MeOH; $[\alpha]^{25}_D$ = +16.0° (*c* 0.45, MeOH); ^{1}H NMR (300 MHz, DMSO-d_6) δ 11.34 (br s, 1H), 7.87 (d, *J* = 7.6 Hz, 2H), 7.72 (d, *J* = 7.3 Hz, 2H), 7.67 (d, *J* = 7.9 H, 2H), 7.41 (t, *J* = 7.0 Hz, 2H), 7.32 (dd, J_1 = 7.3 Hz, J_2 = 7.6 Hz, 2H), 6.63 (br s, 1H), 5.57−5.60 (dd, J_1 = 7.90 Hz, J_2 = 1.51 Hz, 1H, NH), 5.10 (s, 2H, 2 × H-1‴), 4.17−4.28 (m, 4H, H-2, 2 × H-10″, H-9″), 3.76 (d, *J* = 5.5 Hz, 2H, 2 × H_3); ^{13}C NMR (75.4 MHz, DMSO-d_6) δ 167.3, 159.6, 152.0, 147.1 (C-6′), 140.8, 140.7, 139.8, 136.7, 135.1, 124.0, 123.6, 123.0, 121.3, 121.2, 121.0, 120.8, 120.7, 116.2, 116.1, 116.0, 97.7 (C-5′), 72.4 (C-1‴), 64.1, 61.8, 50.1, 42.6. HRMS (FAB, CsI/NaI/glycerol matrix) *m*/*z*, calcd for $C_{23}H_{21}N_3O_7$ $[MH]^+$ 452.1458, obsd 452.1478.

General Method for Preparation of Fully Deprotected Nucleoamino Acids (14−16). Approximately 100 mg of the protected nucleoamino acid (**6**, **10**, or **13**) was dissolved in a solution of 2% DBU in DCM (10 mL). The reaction mixture was stirred for 5 min when TLC analysis showed the disappearance of the starting material. The reaction mixture was concentrated to 4 mL, and 10 mL of H_2O was added. The water layer was washed with $CHCl_3$ (4 × 20 mL) and evaporated to an oily residue. The oil was treated with TFA solution (95% in H_2O, 4 mL) and stirred for 45 min. After TFA evaporation and diethyl ether addition, the product was precipitated as a white solid, which was further washed with ether (4 × 5 mL). **H−Ser^T-OH (14)** (obtained as a 1.5:1 mixture of **14** and DBU−TFA salt). ^{1}H NMR (500 MHz, D_2O) δ 7.50 (q, *J* = 2 Hz, 1H, H-6′), 5.19 (AB quartet, J_{AB} = 18.0 Hz, 2H, 2 × H-1‴), 4.23 (t, *J* = 5 Hz, 1H, H-2), 4.07 (dd, J_1 = 17.5 Hz, J_2 = 6.0 Hz, H-3a), 4.00 (dd, J_1 = 18.5 Hz, J_2 = 5.5 Hz, H-3b), 1.85 (d, *J* = 2 Hz, 3H, CH_3); ^{13}C NMR (125.7 MHz, D_2O) δ 169.5 (C-1), 166.6 (C-4′), 152.3 (C-2′), 141.3 (C-6′), 76.8 (C-1‴), 65.9 (C-3), 52.8 (C-2), 10.80 (*C*H_3). **H−Ser^C-OH (15)** (obtained as a 1:1 mixture of **15** and DBU−TFA salt). ^{1}H NMR (500 MHz, D_2O) δ 7.85 (d, *J* = 8.0 Hz, 1H, H-6′), 6.15 (d, *J* = 7.5 Hz, 1H, H-5′), 5.25 (m, 2H, 2 × H-1‴), 4.28 (t, *J* = 3.5 Hz, 1H, H-2), 4.10 (dd, J_1 = 10 Hz, J_2 = 4.0 Hz, H-3a), 4.04 (dd, J_1 = 11 Hz, J_2 = 3.0 Hz, H-3b); ^{13}C NMR (125.7 MHz, D_2O) δ 169.1 (C-1), 159.6 (C-4′), 149.0 (C-2′), 148.2 (C-6′), 94.9 (C-5′), 78.0 (C-1′), 66.1 (C-3), 52.5 (C-2). **H−Ser^U-OH (16)** (obtained as a 3:1 mixture of **16** and DBU−TFA salt). ^{1}H NMR (500 MHz, D_2O) δ 7.66 (d, *J* = 8.5 Hz, 1H, H-6′), 5.83 (d, *J* = 8.5 Hz, 1H, H-5′), 5.21 (AB quartet, J_{AB} = 10.5 Hz, 2H, 2 × H-1‴), 4.28 (t, *J* = 3 Hz, 1H, H-2), 4.11 (dd, J_1 = 10.5 Hz, J_2 = 4.2 Hz, H-3a), 4.04 (dd, J_1 = 10.5 Hz, J_2 = 3.3 Hz, H-3b); ^{13}C NMR (125.7 MHz, D_2O) δ 169.7 (C-1), 166.6 (C-4′), 152.4 (C-2′), 145.8 (C-6′), 102.3 (C-5′), 77.1 (C-1‴), 65.8 (C-3), 52.5 (C-2) (In all cases, signals from DBU are not reported).

2. αPNA Synthesis, Purification and Analysis. Reagents and Materials. Dimethyl sulfoxide (DMSO) was kept over oven-dried 4 Å MS for at least 12 h before use. 1-Methyl-2-pyrrolidinone (NMP) and *N*,*N*-dimethylformamide (DMF) were distilled under reduced pressure and kept over 4 Å MS for at least 12 h before use. *N*,*N*-diisopropylethylamine (DIPEA) was distilled from CaH_2 (0−1 mm grain size) and kept over 4 Å MS for 12 h before use. Piperidine, DCM, TFA, 1,8-diazabicyclo[5.4.0]undec-7-ene (DBU), diisopropylcarbodiimide (DIC), *N*-hydroxybenzotriazole (HOBt) hydrate, and acetic anhydride were used as received from Aldrich. All amino acids, their derivatives, and Rink Amide MBHA resin (4-(2′,4′-dimethoxyphenyl-Fmoc-aminomethyl)-phenoxy-acetamido-norleucyl-MBHA resin, 0.3−0.8 mmol/g loading capacity, 100−200 mesh) were obtained from Novabiochem. *O*-(7-azabenzotriazol-yl)-1,1,3,3-tetramethyluronium hexafluorophosphate (HATU) was obtained from PerSeptive Biosystems (Applied Biosystems).

Automated Solid-Phase Synthesis Protocol. The synthesis of αPNA was performed on an ACT90 peptide synthesizer (Advance Chemtech) on a 54 μmol scale. During the couplings, 1.2 equiv of amino or nucleoamino acids were used with respect to HATU to prevent tetramethylguanidinium capping.[61] After Fmoc cleavage, the NMP wash is necessary to remove all DBU from the resin. The mixture of acetic anhydride, DIPEA, and DMF was freshly prepared for the capping reaction.

Fmoc Deprotection. a. Resin treated with 2% DBU in DMF (v/v) and mixed for 8 min.

b. Resin washed with DMF (1 × 25 mL DMF-flush; 1 × 10 mL DMF, 1 min shake−flush) followed by NMP (3 × 10 mL, 1 min shake−flush).

Amino Acid Coupling. a. Fmoc-protected amino/nucleoamino acids (3.6 equiv relative to the loading capacity of resin) were preactivated by mixing with HATU (3.0 equiv) and DIPEA (9.0 equiv) in 4/1 NMP−DMSO for 1 min. Final amino/nucleoamino acid concentration was 0.2 M. Fmoc-Cys^{Acm}-OH (6.0 equiv) was preactivated by mixing HOBt hydrate (4.0 equiv) and DIC (4 equiv) in 1:1 DMF−DCM for 5 min.

b. Preactivated Fmoc-protected amino/nucleoamino acid was added to the resin and shaken with N_2 bubbling for 45 min.

(61) Alewood, P.; Alewood, D.; Miranda, L.; Love, S.; Meutermans, W.; Wilson, D. *Methods Enzymol.* **1997**, *289*, 14.

c. The resin was washed with DMF (1 × 25 mL, flush; 3 × 10 mL, shake−flush).

d. Coupling efficiency monitoring: The conventional Kaiser (ninhydrin) test[62] is not ideal for monitoring the solid-phase synthesis of αPNA. It was observed that once the nucleoamino acids are loaded onto the resin the test is always slightly positive (light blue), even after double or triple couplings. Fmoc-counting is the method of choice for monitoring coupling efficiency and can be done by measuring the UV absorbance of the dibenzofulvene chromophore ($\epsilon = 7800\ M^{-1}\ cm^{-1}$ at 301 nm) released upon the Fmoc cleavage by a 20% (v/v) solution of piperidine in DMF. Generally, a single HATU mediated coupling was sufficient for all natural and nucleoamino acids.

N-Capping (acetylation). a. A mixture of Ac_2O (0.5 mL) + DIPEA (0.85 mL) + DMF (4.0 mL) was added to the resin and shaken for 15 min.

b. Resin washed with DMF (3 × 10 mL, 1 min shake−flush) and then DCM (2 × 15 mL, 1 min shake−flush).

Cleavage from Resin. After solid-phase synthesis, the resin was treated with 95% TFA in water (v/v) [3 mL for 100 mg of resin] at room temperature for 1 h, with occasional shaking and sonication. The orange red solution obtained was filtered through glass-wool, and the resin was washed with 95% TFA in water (5 × 1 mL for 100 mg of resin). TFA solution was evaporated on a rotary evaporator at RT to give an orange oil (1−2 mL). Cold ether (ice/water) was added to this orange oil with mixing until an off-white precipitate formed which was washed with ether (5 × 3 mL) and purified as described below.

Analysis and Purification. All crude αPNAs and peptides obtained after resin cleavage were filtered through a cartridge (0.5 × 3 cm) of C18 resin (eluted with 0.1% TFA in 9:1 CH_3CN-H_2O) or Sephadex G-10 gel (eluted with 0.1% TFA H_2O) to remove the nonpeptide impurities. Buffers: A = 0.1% aqueous TFA, B was 0.1% TFA in CH_3CN, C = 100 mM TEAA (triethylammonium acetate), pH 7.2; D = 100 mM TEAA, 20% CH_3CN, pH 7.2), E = 8 mM NaH_2PO_4 in 9:1 water−CH_3CN, pH adjusted to 4 by addition of dilute HCl, F = E + 0.4 M NaCl. αPNA detection wavelength was 254 nm.

Chromatographic Analysis. Analytical HPLCs were performed on a XTerra RP_{18} column (Waters, 3.5 μm 4.6 × 50 mm). A linear gradient of buffer A and B with of 2% increment in buffer B/min and flow rate of 1 mL/min was used. Buffers C and D were used for αPNAs that showed inferior resolution and/or peak broadening in buffers A and B. In general, sufficiently pure 21 mer αPNAs (>60% by HPLC) were obtained after cleavage from the resin.

Semipreparative and Preparative Scale Purification. For a typical αPNA purification, a Water's XTerra RP_{18} (7 μm, 19 × 150 mm) column was used. Similar A−B or C−D buffer-gradients at a flow rate of 15 mL/min were used. Typically 5−6 mg of the crude sample was purified at a time. An absorbance unit (AU) setting (Varian's dual flow cell UV-detector) of 5 was used during the separation for optimal performance. Preparative scale HPLC purifications were performed with a C18−Nucleosil (7 μm, 50 × 250 mm) column. Crude αPNA obtained from a 54 μmol scale synthesis was purified in one run. The same gradient as the semipreparative HPLC was used with a flow rate of 30 mL/min. An AU of 20 is generally the correct setting to obtain a full-scale chromatogram.

Dimerization of αPNAs. Dimerization of backbone 2 αPNAs was achieved by mixing vigorously a solution of αPNA (2.5 mM) in 0.5 M HCl with I_2 in methanol (2 equiv of a 73 mM solution) for 30 min. The reaction mixture was filtered through a Sephadex-G10 gel to remove I_2, followed by a strong cation exchange HPLC purification and desalting by C18 reverse phase HPLC. The same conditions apply for the backbone 1 αPNAs; however, the presence of HCl was not necessary. HPLC conditions: Vydac 400VHP575 SCE column. Linear E−F gradient at 3.33% increment in F/min, flow rate = 1 mL/min). Desalting conditions: XTerra RP_{18} (7 μm, 19 × 150 mm) column, flow rate = 15 mL/min, 0−15 min 100% A, 15−30 min 0−100% B.

Mass Spectral Analysis. MALDI-TOF mass spectra were recorded on a Kratos Kompact MALDI-TOF mass spectrometer. A 1:1 mixture of the sample and the sinapinic acid matrix were run in a linear mode, and the spectrometer was calibrated with insulin as internal standard. Electrospray mass data were recorded on a Micromass Quattro II triple-quadrupole ESI mass spectrometer. Observed masses were derived from the mass of multicharged species using MaxEnt and Transform software packages. The standard deviation value in the observed mass originated during such calculations is not a reflection of measurement-error and only represents upper and lower limits of the calculated values. Mass data for the αPNAs described in this paper are collected in Tables S1 and S2.

3. Binding Studies. Materials. ssDNA was obtained from various companies: Cybersyn Inc., Operon Technology, and Integrated DNA Technology. The commercial oligonucleotides were purified if their purity was less than 95% by analytical HPLC. For a typical reversed-phase HPLC analysis of DNA, an XTerra RP_{18} column (3.5 μm, 4.6 × 50 mm) was used. The mobile phase was composed of buffer A (0.1 M triethylammonium acetate (TEAA), pH 7.2) and buffer B (0.1 M TEAA, 20% acetonitrile, pH 7.2), with a linear gradient of B in A (5 to 95% B in 25 min). Flow rate: 1 mL/min. Detection wavelength: 254 nm. For a semipreparative purification, an XTerra RP_{18} column (Waters, 7 μm, 19 × 150 mm) was used with the same gradient as the analytical system and a flow rate of 15 mL/min. The concentrations of αPNA solutions were determined by UV absorbance using the nearest neighbor approximation[63] assuming that the extinction coefficients of the nucleobases in αPNAs are the same as in DNA. Concentration of abasic (control) peptide was determined by quantitative ninhydrin analysis.[64]

UV Melting Experiments. For b1 αPNA, thermal UV denaturation curves were obtained with sample solutions made by combining the αPNA and ssDNA components (final concentration was 5 μM in each oligomer) in HPLC grade water followed by heating at 75 °C for 5 min and then cooling and storage at 4 °C for 4 days. For b2 αPNA, thermal UV denaturation curves were obtained with sample solutions made by combining the αPNA and ssDNA components (final concentration was 5 μM in each oligomer) in TE buffer (10 mM Tris-HCl, 1 mM EDTA, pH 7) followed by heating at 75 °C for 5 min and then cooling and storage at 4 °C for overnight. All measurements were conducted in a 1-cm path length quartz cell equipped with a temperature probe. The absorbance at 260 nm was recorded as a function of temperature using a Perkin-Elmer Lambda 20 UV/VIS spectrophotometer equipped with a PTP-1 Peltier system thermocontroller with heating/cooling rates of 1 °C/min over the range of 5 to 75 °C. Below 20 °C, dry N_2 gas was passed through the spectrophotometer sample chamber to prevent moisture condensation. Data were collected and evaluated using the TempLab software package. The melting temperature, T_m (defined as the temperature at which 50% of a complex is dissociated into its constituent components) was determined from the inflection point maximum of the first derivative of the melting curves and is the average of two separate runs.

Circular Dichroism Studies. CD spectra were either recorded on a Jasco *J*-600 or *J*-810 spectropolarimeter. CD spectra were the average of eight scans obtained by collecting data at 0.10 nm intervals from 320 to 190 nm, with a response time of 2 s, bandwidth of 1 nm and sensitivity of 20 mdeg. Stoppered optical cells of path length 1 cm were used. Unless otherwise specified, all the samples were constituted with HPLC grade water. For the experiments involving only αPNA, the measured original CD data (expressed as ellipticity $[\theta]_{obs}$: in mdeg) was converted to the optical constant (molar ellipticity). Molar ellipticity is reported as the mean residue molar ellipticity ($[\theta]$, deg·cm^2·dmol^{-1}) and is calculated from the following equation: $[\theta] = [\theta]_{obs}(mrw)/10lc$

(62) Sarin, K. V.; Kent, B. H. S.; Tam, P. J. *Anal. Biochem.* **1981** *117*, 6147.

(63) Puglisi, J. D.; Tinoco, I., Jr. *Methods Enzymol.* **1989**, *180*, 304.

Where mrw is the mean residue molecular weight (molecular weight of the peptide divided by the number of amino acid residues), c is the peptide concentration in grams per milliliter, and l is the optical path length of the cell in centimeter.

For the TTTTT(b1)-dimer, a thermal denaturation profile between 30 and 80 °C was obtained. The helical content at 20 °C was estimated from a separate CD experiments by taking the ratio of $([\theta]_{219} - [\theta]_0)/[\theta]_{100}$, where $[\theta]_{219}$ is the mean residual helicity at 219 nm ($= -14\,850$ deg·cm^2·dmol^{-1}), $[\theta]_0$ is the "background" mean residue ellipticity at 0% helicity ($= -5368$ deg·cm^2·dmol^{-1}) as determined by a melting experiment. To account for the length dependence of CD for an α-helix, the following formula was used to calculate $[\theta]_{100}$;[65] $[\theta]_{100} = [\theta]_H^{\infty}(1 - k/n)$. Where $[\theta]_H^{\infty}$ is the molar ellipticity for an infinite helix ($-38\,400$ deg·cm^2·dmol^{-1}), k is a wavelength-dependent factor ($= 2.69$), and n is the number of residues in the helix ($= 42$). The α-helix percentage in the structure was determined to be 26% by taking the ratio of $[\theta]_{219}$(obs)/$[\theta]_{219}$(100% helix).

Gel Mobility Shift Experiments. Solutions were made by combining DNA (300 pmole) with varying amounts of αPNA in 7.5 μL of TE-buffer followed by heating at 75 °C for 5 min and then cooling and storage at 4 °C for overnight. Before electrophoresis, 2.5 μL of loading buffer (0.01% xylene cyanol FF, 0.01% bromophenol blue solution, 60% (w/v) glycerol in 44 mM Tris-borate, pH 7.2) was added to the sample and mixed. An amount of 3.5 μL of the sample was loaded onto the gel. Free and αPNA bound DNA were resolved by nondenaturing 14% polyacrylamide gel electrophoresis in 44 mM Tris-borate, pH 7.2 for 1 h at 14 V/cm at 4 °C. The gel was visualized by silver stain using the PlusOne DNA silver staining kit (Pharmacia Biotech).

Determination of Dissociation Constant (K_d) by Gel Shift Assay. For determination of K_d, the following equation was assumed for DNA (D) and αPNA (P) interaction to form the complex αPNA−DNA (DP): D + P ↔ DP; The concentrations of bound and free DNA, $[D_b]$ and $[D_f]$ respectively, can then be related to equilibrium constant: $K_d = [D_f]([P_o] - [D_b])/[D_b]$; $[P_o]$ and $[D_o]$ are the total concentration of αPNA and DNA, respectively. In the gel shift experiment, the total concentration of DNA was fixed (30 μM) and the concentration of αPNA was varied. ρ is defined as the molar ratio of the αPNA and DNA ($[P_o] = \rho[D_o]$). $[D_b]$ was determined from the intensity of the silver stained gel band corresponding to the retarded αPNA−DNA complex using Quantity One software (Bio-Rad). It is assumed that no dissociation of the αPNA−DNA occurs during electrophoresis. K_d was obtained by plotting either ρ against $[D_b]$ or $1/([D_o] - [D_b])$ against ρ/D_b (linear plot) using the following equation: $\rho/[D_b] = K_D/\{[D_o]-([D_o] - [D_b])\} + 1/D_o$.

Sample Preparation for the NMR Experiments. DNA d(A_3-GGAGGA_3) and the αPNA CCTCC (b2) were used for the NMR experiments. The recommended concentration of the individual oligomer strands (αPNA and ssDNA) for one- and two-dimensional NMR experiments is 0.5−1 mM for a superior signal-to-noise ratio. The acidity of the αPNA solution obtained directly from the purification by HPLC in TFA buffer was adjusted by addition of NH_4HCO_3 solution (1 M, 4 equiv to αPNA concentration) and lyophilization of the resulting solution. The resulting white powder was dissolved in water and re-lyophilized for four times before the final solution was made. Commercially available ssDNA was purified by HPLC using a C18 column and TEAA buffer system first, and then the excess TEAA was exchanged with ammonium bicarbonate. The buffer exchange was accomplished by a C18 chromatography using an elution gradient of 10 mM NH_4HCO_3 solution versus CH_3CN. The column was eluted first with 100% 10 mM NH_4HCO_3, pH 8.0 for 10 min, then ramped to 100% Buffer B (10 mM NH_4HCO_3, 20% CH_3CN, pH 8.2.) within 30 min. The resulting ssDNA solution was lyophilized in manner similar to αPNA, as described above, before making the final solution. Samples of ssDNA and αPNA obtained from the above sources were individually reconstituted with a 20 mM sodium phosphate buffer solution (pH 7.0, 95:5 water−D_2O mixture), and mixed together.

NMR Spectroscopy. All NMR spectra were recorded on a Varian Inova 600 spectrometer equipped with a triple-resonance gradient probe. Unless stated otherwise, the spectra were recorded at a probe temperature of 5 °C. All experiments were performed with WATERGATE water suppression.[66] The NMR data were processed and analyzed using the program FELIX 98 (Molecular Simulations, Inc.).

Acknowledgment. This work was supported by grants from the National Institutes of Health (GM-54796) and by the Center for AIDS Research at Case Western Reserve/University Hospitals of Cleveland (AI-36219). Thanks to the Orlando Research Group (Complex Carbohydrate Research Center, University of Georgia) for performing the MALDI-TOF mass spectrometry and Dale Ray (Case) for assisting us with HMBC/HMQC NMR experiments. Special thanks Prof. Tony Berdis, Prof. Irene Lee, Prof. Peter DeHaseth, and Gianina Panaghie for technical assistance and helpful comments.

Supporting Information Available: MS data for all new compounds and experimental protocols for the αPNA−ssDNA binding studies. This material is available free of charge via the Internet at http://pubs.acs.org/.

JA038434S

(64) Sarin, V. K.; Kent, S. B.; Tam, J. P.; Merrifield, R. B. *Anal. Biochem.* **1981**, *117*, 147.
(65) Chen, Y.; Yang, J. T.; Chau, K. H. *Biochemistry* **1974**, *13*, 3350.
(66) Piotto, M.; Saudek, V.; Sklenar, V. *J. Biomolecular NMR* **1992**, *2*, 661.